

A SIMPLE METHOD TO ANALYZE AND PREDICT SHAFT MISALIGNMENT  
IN MARINE VESSELS

A Thesis

Presented in Partial Fulfillment of the Requirements for the

Degree of Master of Science

with a

Major in Mechanical Engineering

in the

College of Graduate Studies

University of Idaho

by

Daniel P. Keane

April 2014

Major Professor: Edwin Odom, Ph.D., PE

## Authorization to Submit Thesis

This thesis of Daniel Keane, submitted for the degree of Master of Science with a Major in Mechanical Engineer and titled "A Simple Method to Analyze and Predict Shaft Misalignment in Marine Vessels," has been reviewed in final form. Permission, as indicated by the signatures and dates given below, is now granted to submit final copies to the College of Graduate Studies for approval.

Major Professor \_\_\_\_\_ Date \_\_\_\_\_

Edwin Odom, Ph.D.

Committee

Members \_\_\_\_\_ Date \_\_\_\_\_

Matthew Riley, Ph.D.

\_\_\_\_\_ Date \_\_\_\_\_

Carla Egelhoff, Ph.D.

Department

Administrator \_\_\_\_\_ Date \_\_\_\_\_

John Crepeau, Ph.D.

Discipline's

College Dean \_\_\_\_\_ Date \_\_\_\_\_

Larry Stauffer, Ph.D.

Final Approval and Acceptance by the College of Graduate Studies

\_\_\_\_\_ Date \_\_\_\_\_

Jie Chen, Ph.D.

## **Abstract**

This thesis demonstrates the practical application of a generalized method to solve for beam deflection. Castigliano's theorem is augmented through the use of the method of Lagrange Multipliers to solve nearly any beam deflection problem. This novel method, first developed by the late Dr. Ju of the University of New Mexico, is used as the foundation to develop a simple tool to solve a marine propulsion shaft alignment problem. This method proved to be computationally inexpensive and the program can be run on nearly any computer. An optimization code determines the optimal bearing offsets which allow the shaft alignment to satisfy predetermined alignment constraints. Experimental validation of the computer model's predicted deflection results were promising, with model deflection results within 10% of experimental values.

## **Acknowledgments**

I would like to thank my thesis board members, Dr Edwin Odom, Dr. Carla Egelhoff and Dr. Matt Riley for their time and efforts in helping this thesis to complete.

I would like to give a special thanks to Dr. Egelhoff for taking the time to drive all the way from Butte, Montana to attend my thesis defense.

## Table of Contents

Authorization to Submit Thesis .....	ii
Abstract .....	iii
Acknowledgments .....	iv
Table of Contents .....	v
List of Tables .....	ix
Chapter 1. Introduction .....	1
1.1 Overview .....	1
1.2 Thesis Objectives .....	1
1.3 Thesis Organization .....	1
1.4 Propulsion System Basics .....	2
1.4.1 System Description and Configurations .....	2
1.4.2 System Design .....	4
1.4.3 Propulsion Shaft Alignment: .....	5
1.4.4 Methods of Measuring Bearing Reactions: .....	8
Chapter 2. Dr. Ju's Method for Solving Beam Deflections .....	11
2.1 Introduction .....	11
2.2 Analytical Approach .....	11
2.2.1 Beam Deflection Analysis .....	11
2.2.2 Castigliano's 2 <sup>nd</sup> Theorem .....	12
2.2.3 Method of Lagrange Multipliers .....	13
2.3 Dr. Ju's Method .....	15
2.3.1 Theory .....	15
2.3.2 Example Problem .....	16
2.3.3 Modeling of the End Reaction/Engine Connection .....	18
Chapter 3. Optimization of Bearing Offsets .....	21
3.1 Introduction to Optimization Theory .....	21
3.1.1 Optimization Methods .....	21
3.1.2 Optimization of Bearing Offsets .....	22
3.1.3 Standard Optimum Form: .....	23

3.1.4	Description of Design Variables, Constraints and Objective Functions .....	25
3.1.5	Exterior Penalty Method with Steepest Descent Method .....	27
3.2	Optimization Code Description .....	29
3.3	Development of Function Approximations .....	30
3.4	Results .....	31
3.5	Conclusions.....	33
Chapter 4.	Methodology and Data Collection.....	34
4.1	Overview.....	34
4.2	Methodology .....	34
4.2.1	Model System .....	34
4.2.2	Scaling of the Propulsion System .....	34
4.2.3	Experimental Model Fabrication .....	36
4.2.4	Test Configurations.....	38
4.3	Deflection Measurement .....	40
4.3.1	Experimental Procedure .....	40
4.3.2	Computer Model Data Preparation.....	40
4.4	Data Collection .....	41
4.4.1	Experimental Error .....	41
4.4.2	Experimental Results .....	42
Chapter 5.	Conclusions and Recommendations .....	49
5.1	Conclusions.....	49
5.2	Future Work and Recommendations .....	49
References.....		50
Appendix A: TKSolver Shaft Deflection Code .....		52
Precalc Function: .....		53
Reactions Function .....		56
Display Results Function.....		56
Mx Function.....		56
DEFL Function.....		56
Appendix B: MATLAB Optimization Code.....		57
First Iteration Code.....		58

Second Iterations with Revised Function Approximations ..... 63

Appendix C: Matrix used for Calculation in TKSolver Shaft Model ..... 69

## List of Figures

Figure 1: Components of a multi-section shaft coupled to a reduction gear. ....	2
Figure 2: A directly coupled shaft/engine arrangement. ....	3
Figure 3: A typical twin screw set up. ....	3
Figure 4: Desired Tail Shaft Contact Area. [2] ....	6
Figure 5: Locations to be checked by filler gauge to determine misalignment angles. ....	6
Figure 6: Dial Indicator position to check crank web deflection. ....	7
Figure 7: Example of gear contact dye test, showing misalignment. ....	7
Figure 8: Sagging is defined as opening of the crank throw at top-dead center (TDC) [6]. ....	8
Figure 9: Positions for hydraulic jack and dial indicator during a jack-up procedure to determine bearing load. ....	9
Figure 10: Strain gauge diagram set up in a Wheatstone bridge configuration ....	10
Figure 11: A linear-elastic Stress-Strain Curve. ....	12
Figure 12: Free Body Diagram for the Shaft. ....	16
Figure 13: Full Scale Deflection Results. ....	35
Figure 14: Scaled (1/8) Deflection Results. ....	35
Figure 15: An Old Bridgeport Mill Base was used as the Experiment Test Bed ....	36
Figure 16: Initial Modeled Engine End Connection ....	37
Figure 17: Final Engine End Connection Model. ....	37
Figure 18: First Experimental Set up (steel tube). ....	38
Figure 19: Configuration for Rectangular Bar Test. ....	39
Figure 20: Point Load Bearing. ....	40
Figure 21: Plot of 4130 Steel Tube Experimental and Model Deflections ....	42
Figure 22: Shaft Run-out for 4130 Steel Tube ....	44
Figure 23: Plot of 1018 Steel Rod Model and Experimental Deflections ....	45
Figure 24: Plot of C110 Copper Bar Model and Experimental Deflections ....	47

## List of Tables

Table 1: Function Approximation Errors .....	31
Table 2: Initial Bearing Reactions .....	31
Table 3: Final Bearing Reactions (non-discrete offsets) .....	32
Table 4: Final Bearing Reactions (Discrete Offsets).....	32
Table 5: Results for the 4130 Steel Tube (2.205 lbs).....	43
Table 6: Results for the 4130 Steel Tube (4.41 lbs).....	43
Table 7: Results for the 1018 Steel Rod (2.205 lbs).....	45
Table 8: Results for the 1018 Steel Rod (4.41 lbs).....	46
Table 9: Results for the Copper Bar (2.205 lbs).....	47
Table 10: Results for the Copper Bar (4.41 lbs).....	48

## **Chapter 1. Introduction**

### **1.1 Overview**

This thesis investigates a novel method in solving for beam deflection, slope and reaction forces. This novel method combines Castigliano's second theorem and the method of Lagrange Multipliers and was first proposed by Dr. Ju of the University of New Mexico in his paper, "On the Constraints of Castigliano's Theorem" in 1971 [1]. The effectiveness of this method will be demonstrated by using it to model the deflection an actual propulsion system on a ship. The ultimate goal is to develop an accessible and easy to use shaft model and optimization tool which can be used to check shaft alignment and predict the best case bearing offsets for various vessel operating conditions.

### **1.2 Thesis Objectives**

The objectives of this thesis are listed below:

- Demonstrate the effectiveness Dr. Ju's method
- Validate this method experimentally
- Develop an easy to use and computational friendly model to predict shaft deflections and bearing loads.
- Determine the optimal bearing offsets for various loading conditions

### **1.3 Thesis Organization**

This thesis is organized into six chapters. Chapter 1 introduces the thesis objectives and reviews current literature concerning shaft alignment. Chapter 2 introduces Dr. Ju's method and the mathematic and mechanical theories supporting his method. Chapter 3 discusses optimization of bearing offsets to accommodate different operating conditions. Chapter 4 includes and analysis of the experimental data and computer model predictions. Chapter 5 includes the conclusions and recommendations followed by a list of references used in the analysis.

## 1.4 Propulsion System Basics

### 1.4.1 System Description and Configurations

The most important and perhaps most complex mechanical system onboard a ship is the propulsion system. After all, without it, the ship becomes merely a floating steel container. Reduced to its basic components, this system typically includes one or more prime movers (diesel engines, turbines, etc.) coupled to a reduction gear system, a propeller shaft, propeller and bearings. Power and torque generated by the main propulsion engine is used to turn the propulsion shaft, which turns a propeller at its end.

Propulsion systems take numerous forms depending on the size and purpose of a vessel. Figure 1 shows a typical single-shaft configuration from the output of the reduction gear to the propeller, including bearing locations. This configuration represents a medium-sized container vessel, which usually requires its engine revolutions per minute (rpm) to be reduced to a usable speed via a reduction gear/gearbox.[2]

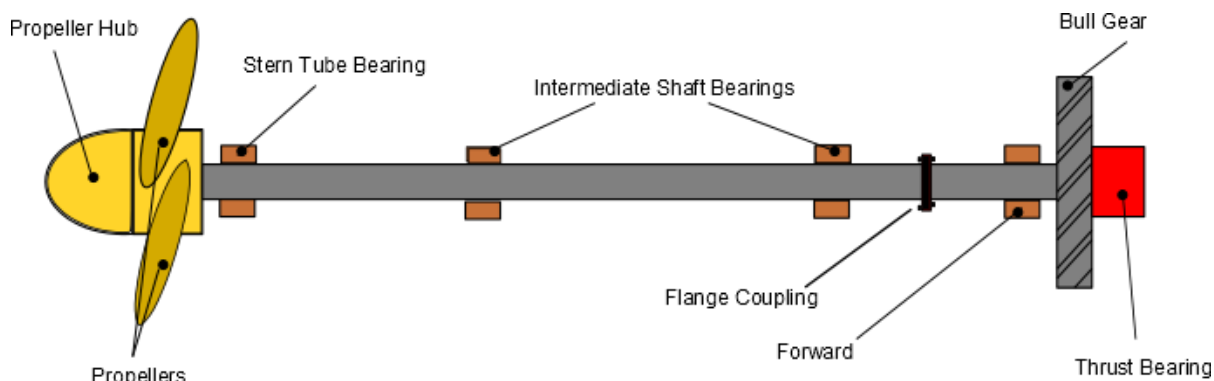


**Figure 1: Components of a multi-section shaft coupled to a reduction gear.**

Large Oil Tankers, sometimes referred to as Ultra Large Crude Carriers (ULCC) or Very Large Crude Carriers (VLCC) depending on their displacement, often directly couple their large slow speed marine diesel engine to the propulsion shaft. [2] Proper shaft alignment is extremely critical for these vessels since unusual bending moments or shear forces are directly transferred to the aft engine bearings.[3] Depending on hull deflection and engine bed-plate sagging these bearings can become unloaded and transfer their loads to the next forward most bearing.[3] Edge loading and eventual bearing failure may soon follow. Since

they usually only have one shaft, an equipment casualty to the shaft line or engine will leave the vessel dead in the water.

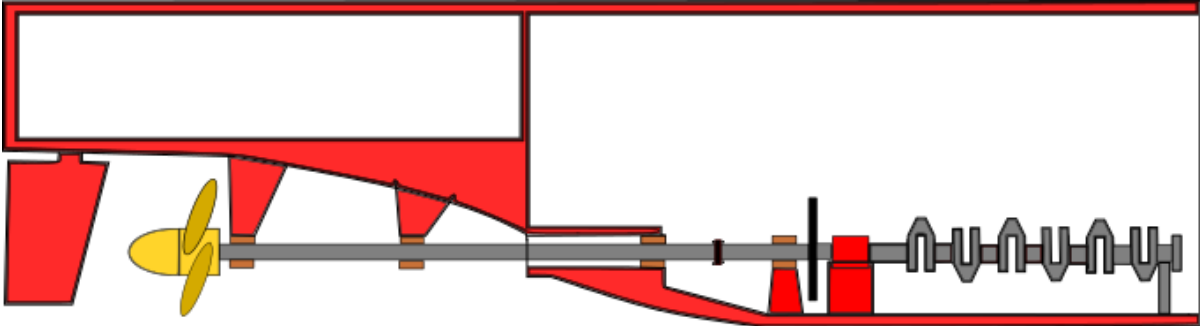


**Figure 2: A directly coupled shaft/engine arrangement.**

Smaller vessels will have multiple engines and shafts. If multiple shafts are used, then the stern tube bearing is moved forward and struts are used to support the shaft so that the propeller can be moved to a usable location without creating a non-hydrodynamic hull shape.

[4]



**Figure 3: A typical twin screw set up.**

Note the rudders positioned directly behind the propellers and also the amount of exposed shaft, supported by struts.

### 1.4.2 System Design

A critical component in maintaining a vessel's propulsion system is proper shaft alignment. Numerous forces act on the propeller shaft while the ship is in motion. Forces transmitted along the shaft axis, generated by the propeller, act on a thrust bearing on the forward end of the shaft and drive the ship forward through the water. Hull motion due to sea state (wave height and wind speed) causes the hull to deform, which in turn, causes stress on the propeller shaft. Side forces are generated by the propeller as it turns through the water causing a bending moment on the shaft. [5]

All propulsion system designs fall into one of three categories: [3]

- (1) A stiff hull with a propulsion shaft design of similar stiffness (typical of smaller vessels). In this case, with both the system and shaft having similar stiffness, any deflection of the hull will be nearly identical to that of the shaft, resulting in almost no relative change in bearing offset or bearing loadings. This system is compliant with American Bureau of Shipping Standards. [2]
- (2) A stiff propulsion system with a significantly less stiff hull (not desirable). In the second case, a stiff propulsion shaft with an elastic hull will result in a system which is very susceptible to hull deflections. Because the shaft will not deform with the structure of the ship, bearing offsets and load will change greatly, resulting in possible bearing failure.
- (3) A stiff hull with a less stiff propulsion system (desired design). This case is similar to case one, only the shaft will maintain in contact with the bearings no matter how the hull flexes.

Shaft alignments are done almost exclusively while the ship is in dry-dock. This poses several problems.

First, shaft alignment changes as soon as the ship is placed in the water. The buoyant force of the water supports the hull differently from the dry-dock causing the hull to deflect under the changed load. The ship is at ballast condition when first refloated. Ballast condition is the lowest possible liquid load state where the ship can be safely moved to and from dry-dock without stability being critical. A vessel's liquid load always includes propulsion fuel,

lubrication oil, hydraulic oil and potable water. It also may include ballast water, aviation fuel, and cargo liquids depending on the vessel's purpose.

Next, by nature the ocean is a dynamic environment. An ocean going vessel is never truly in calm waters. Because the ship's hull is usually stiffer than the shaft, any local hull deflections are carried into and reflected in the shaft.

Also temperature variations within the system will affect alignment. Individual bearing offsets both inside the engine and along the shaft line are particularly susceptible to temperature change.

In order to account for these conditions naval architects seek an optimal alignment which gives the best possible set of bearing offset positions which meet alignment requirements in both ballast and laden conditions.

### **1.4.3 Propulsion Shaft Alignment:**

Shaft alignment is defined by the American Bureau of Shipping as, "a static condition observed at the bearings supporting the propulsion shafts. In order for the propulsion shafting alignment to be properly defined, the following minimum set of parameters (whichever may be applicable) need to be confirmed as acceptable":[2]

Bearing vertical offset: Bearing offset is vertical displacement of the contact face of the bearing from the established central line of the shafting. Usually the tail shaft bearing and #1 Main engine bearing are designated as a 0" offset since they mark the ends of the shaft line. All of the bearings are positioned horizontally (fore and aft) and vertical to adjust bearing reactions so that they remain positive and within design constraints.

Bearing reactions: Calculations need to show that under maximum allowable alignment tolerances, bearing loads are within specified manufacturer limits and that all reactions are positive. In general, it is very difficult to measure bearing reactions directly. Methods to determine bearing reactions include the use of strain gauges, hydraulic jacks, or numerical methods to reverse-engineer the bearing reactions. ABS loading criteria for metallic bearings is no more than  $0.8 N/mm^2$ . Loading criteria for lubricated synthetic bearings is no more than  $0.6 N/mm^2$ . [2]

The tail-shaft bearing is used as the baseline for the bearing offset. The tail-shaft bearing usually carries the most weight due to the suspended weight of the propeller. Proper alignment and contact area is critical to system reliability. If the calculated relative misalignment slope between the shaft and the tail shaft bearing is greater than  $0.3 \times 10^{-3}$  rad, then the relative misalignment slope should be reduced by means of slope boring or bearing inclination.[2] Figure 3 shows the desired bearing contact area:

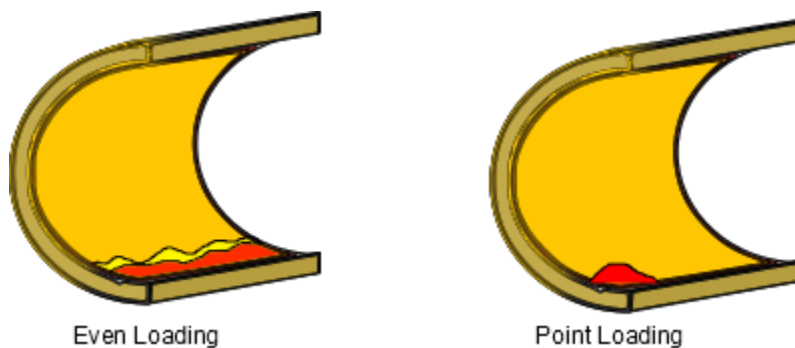


**Figure 4: Desired Tail Shaft Contact Area. [2]**

Misalignment angles: A misalignment at the bearings, which are physically accessible for measurements, is easily evaluated by filler gauges. Horizontal misalignment is measured at the port and starboard side of the bearing, and vertical misalignment is checked at the forward and aft edge of the bearing. Usually the shaft is rotated and measured several times to determine if the misalignment is a result of shaft run-out or actual bearing misalignment.

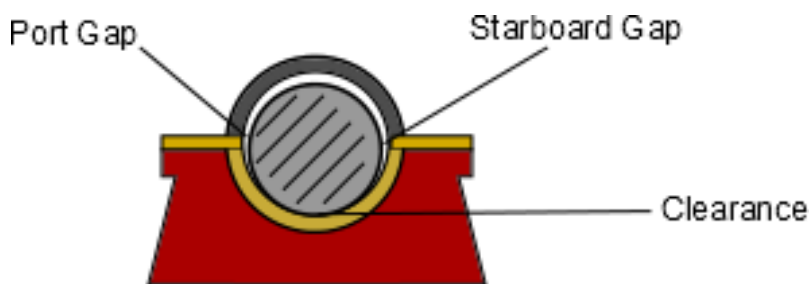


**Figure 5: Locations to be checked by filler gauge to determine misalignment angles.**

Crankshaft's web deflections: Crankshaft web deflections are a method to measure bearing misalignment within the engine or an excessive bending moment imparted by the shaft. A

dial indicator is placed between crank webs for a particular piston. The crank is slowly turned and any change in horizontal distance is recorded. This is an indication of possible shaft misalignment.

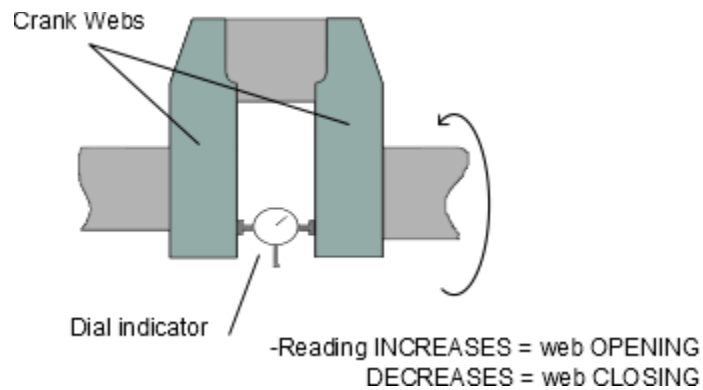


**Figure 6: Dial Indicator position to check crank web deflection.**

Gear misalignment: Another indication of shaft misalignment is lack of contact between gear faces between the bull gear and pinion drive gear in the reduction gear. Gear contact is checked by use of a dyeing agent. If the dye color on a gear face is not even this may indicate a large misalignment.

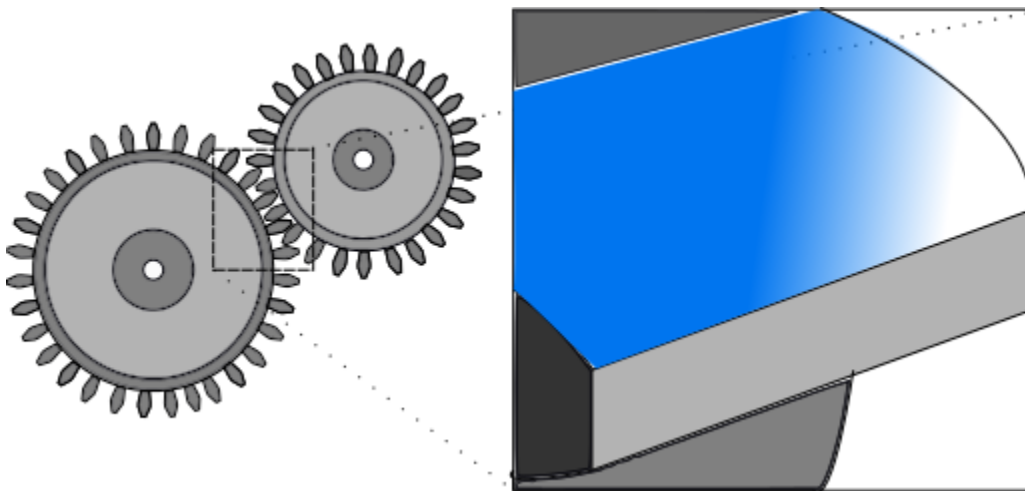


**Figure 7: Example of gear contact dye test, showing misalignment.**

Shaft and bearings' strength: Also calculations need to show that all shear forces and bending moments are within design limits for the shaft and that all forces and moments imparted on propulsion equipment including both reduction gear and propulsion engines are within manufactures limits.

Coupling bolts' strength: Coupling bolt strength must be high enough to absorb all static and dynamic forces imparted on the shaft in shear, torsion or bending from numerous sources including engine torque, hull deflection, propeller side forces and possible misalignments.

Engine Bedplate Sagging: Since the midsection of an engine will expand more than its ends due to thermal expansion, the change in each bearing offset is a function of location. Common practice it to pre-sag the engine bedplate to ensure uniform offset at operating conditions. Sagging is defined as opening of the crank throw at top-dead center (TDC). The crankshaft is allowed to sag at cold iron condition so that at operating conditions the crank shaft is straight and the crank throw is uniform at all rotational positions. [3]

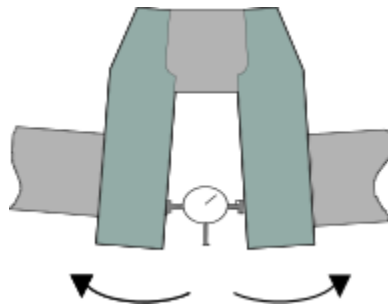


**Figure 8: Sagging is defined as opening of the crank throw at top-dead center (TDC) [6]**

Bearing offset and bearing reactions are usually the critical constraints in shaft alignment. Typically, bending moments and shear stresses are well within design tolerance for the shaft.

#### **1.4.4 Methods of Measuring Bearing Reactions:**

Two methods are used to measure bearing reactions. Strain gauge measurement is an indirect method, while the Jack-up method directly measures bearing reactions. Often a combination of these methods is used depending on the shaft configuration and space restrictions within the engine room. Bearing locations may not be well suited to allow a

hydraulic jack to be positioned to lift the shaft or parts of the shaft may not be accessible to properly position strain gauges.

The jack-up method directly measures the force required to lift the shaft free of the lower bearing surface. In this method a jack is placed either directly forward or aft of the bearing. A load cell is placed between the shaft and the jack and a dial indicator is positioned to show when the shaft begins to lift. Because the jack is not positioned directly under the bearing a correction factor is used to obtain the actual load at the bearing.

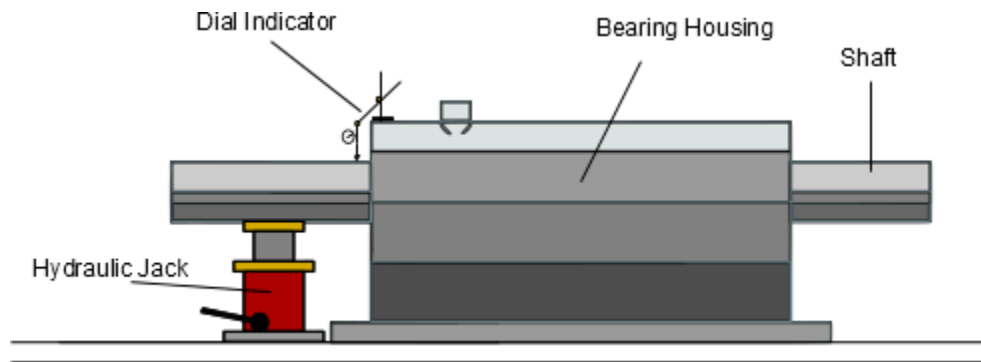


**Figure 9: Positions for hydraulic jack and dial indicator during a jack-up procedure to determine bearing load.**

Strain gauge measurements are extremely useful for sections of the shaft which can't be reached using the jack-up method. Additional advantages include the ability to measure multiple shaft sections at one time, the ability to repeat measurements quickly, and the ability to measure both vertical and horizontal bearing loads. However, accuracy of the strain gauge calculations depends on the system model.[3]

As the shaft deforms when rotated, the strain gauges deform, changing the gauge's resistance. Strain is calculated as follows:

$$\varepsilon = \frac{\Delta R}{R} * \frac{1}{K} \quad (1-1)$$

and

$$\frac{\Delta R}{R} = \frac{V_{out}}{V_{in}} \quad (1-2)$$

Where  $\varepsilon$  is the strain, R is the resistance in ohms, V is voltage in millivolts and K is the bridge factor (usually 2). Strain gauges are usually mounted in a Wheatstone bridge configuration where two pairs of gauges are mounted 180° apart. [7]

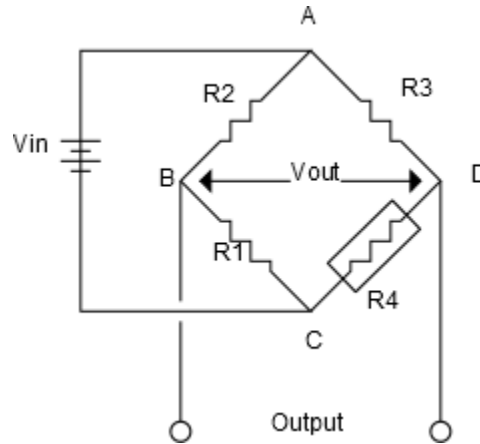


**Figure 10: Strain gauge diagram set up in a Wheatstone bridge configuration**

The shaft's bending moment is calculated using the following equation, where M is the bending moment, E is young's modulus for the shaft material, W is the section modulus and  $\varepsilon$  is the strain calculated above:

$$M = E * W * \varepsilon \quad (1-3)$$

The section modulus for a shaft is:

$$W = \frac{\pi D^3}{32} \quad (1-4)$$

Combining equations 1-1 through 1-4, the moment is:

$$M = E * \frac{\pi D^3}{32} * \frac{V_{out}}{V_{in}} * \frac{1}{K} \quad (1-5)$$

## **Chapter 2. Dr. Ju's Method for Solving Beam Deflections**

### **2.1 Introduction**

This section will cover the theory behind Dr. Ju's method for solving beam deflection. Dr. Ju's method combines Castigliano's 2<sup>nd</sup> Theorem with the Method of Lagrange Multipliers to solve any beam deflection problem. First, the mathematic and mechanical theory behind Castigliano's 2<sup>nd</sup> Theorem and the Method Lagrange Multipliers will be discussed, then Dr. Ju's method will be examined followed by an example problem using his method.

### **2.2 Analytical Approach**

#### **2.2.1 Beam Deflection Analysis**

There are numerous well used and proven methods for determining beam deflection. [8] Some of the most popular include double integration, moment-area theorems, superposition, conjugant beam method and Castigliano's theorem. New methods are constantly being developed. Jong and Rencis developed a Model Formula Method which derived 4 model equations using singularity functions. [8] This method improved on the Method of Segments which Rencis published the year before. [9] An approach described by Prof. Ju of the University of New Mexico, in his paper, "On the Constraints for Castigliano's Theorem." [1], [10] Dr Ju's method improved upon Castigliano's second theorem through the use of the method of Lagrange Multipliers to solve any beam deflection problem. Before Dr. Ju's method is discussed further, a discussion of theories behind both Castigliano's 2<sup>nd</sup> Theorem and the Method of Lagrange Multipliers is required.

### 2.2.2 Castigliano's 2<sup>nd</sup> Theorem

Castigliano's theorem on deflections states that, "If an elastic system is supported so that rigid body displacements of the system are prevented, and if certain concentrated forces of  $F_1, F_2, \dots, F_i$  act on the system, in addition to distributed loads and thermal strains, the displacement component  $q_i$  of the point of application of the force  $F_i$ , is determined by the equation: [11]

$$q_i = \frac{\partial U^*}{\partial F_i} \quad (2-1)$$

Where  $U^*$  is the complementary energy of the system and  $F_i$  is each force acting in the system. Because this equation applies to small displacements for linearly elastic materials,  $U^*$  is approximately equal to  $U$ .  $U$  is the strain energy for the system or the area under the stress strain curve as shown below.[11]

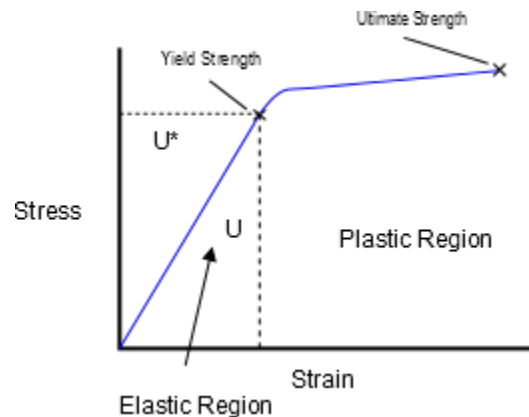


**Figure 11: A linear-elastic Stress-Strain Curve.**

Strain energy generated by a bending moment can be written as:

$$U_m = \int dU_m = \int \frac{1}{2} * M d\phi \quad (2-2)$$

Where  $\frac{M}{2} * d\phi$  is simply the area under the stress strain curve (a triangle) for an element in the system. By making several substitutions based on the geometry of the deformed element:

$$d\phi = \frac{de_z}{y} \quad (2-3)$$

$d\phi$  is the angle of deformation along the surface of the element.  $d\mathbf{e}_z$  is the deformation in the  $z$  direction. In this case,  $z$  is along the axis of the beam.  $y$  is the distance from the center of the centroid of the element.

$$d\mathbf{e}_z = \boldsymbol{\varepsilon}_{zz} dz \quad (2-4)$$

$\boldsymbol{\varepsilon}_{zz}$  is the strain in the  $z$  direction and  $dz$  is the length of the element in the  $z$  direction.

$$\boldsymbol{\varepsilon}_{zz} = \frac{\boldsymbol{\sigma}_{zz}}{E} \quad (2-5)$$

$\boldsymbol{\sigma}_{zz}$  is the stress in the  $z$  direction.  $E$  is Young's Modulus and  $I$  is the moment of inertia.

$$\sigma_{zz} = \frac{M * y}{I} \quad (2-6)$$

We arrive at the strain energy in bending equation in its final form:

$$U_m = \int \frac{M^2}{2EI} dz \quad (2-7)$$

By taking the partial derivatives with respect to Force ( $F_i$ ) and Moments ( $M_i$ ) we have terms for both displacement and slope for the given system.

$$q_i = \frac{\partial U_m}{\partial F_i} = \int_0^L \frac{M}{EI} * \frac{\partial M}{\partial F_i} dz \quad (2-8)$$

$$\theta_i = \frac{\partial U_m}{\partial M_i} = \int_0^L \frac{M}{EI} * \frac{\partial M}{\partial M_i} dz \quad (2-9)$$

The above equations will only supply information for deflection at any point where a concentrated load acts on the system.

In order to determine the deflection at any point in the system a dummy load is used to create a virtual force or moment at the desired location. The partial derivative of the moment equation is taken at that point and then the dummy Moment or Force is set to zero.

### 2.2.3 Method of Lagrange Multipliers

In his book Analytical Mechanics, Lagrange describes to use of undetermined multipliers to change a constrained physical system into an unconstrained system. Lagrange's original purpose was to derive a method which made it easier to solve the equations of equilibrium for a system. His Generalized Equation of Equilibrium:

$$L = Pdp + Qdq + Rdr + \dots + \lambda dL + \mu dM + \nu dN = 0 \quad (2-10)$$

Describes a system where P, Q and R, are defined as the forces acting in a system and  $Pdp$ ,  $Qdq$  and  $Rdr$  are their associated moments. Each force is a function of  $(x, y, z, \text{etc})$ . When the equations of conditions ( $L, M, N$ ) or "constraints" are added to the system, each multiplied by an undetermined multiplier  $(\lambda, \mu, \nu)$ , the result is equilibrium. Each variable may now be treated as independent.[12]

This method is frequently used to find minima or maxima of a function and is usually expressed as:

$$L(x_1, \dots, x_n, \lambda_1, \dots, \lambda_k) = f(x_n) + \lambda_k g_k(x_n) \quad (2-11)$$

The Lagrangian function  $L$ , equals the objective function to be minimize/maximized plus the sum of its  $k$  associated constraint functions, each multiplied by its own undetermined multiplier. If the differential is taken with respect to the  $x_n$  variables and  $\lambda_k$  multipliers, a system of  $n + p$  equations is obtained which can be used to solve for the  $n + p$  unknowns.

A simple example follows:

$$\min f(x) = 4x_1^2 - 3x_2^2 + 2x_1x_2 + 6x_1 - 3x_2 + 5 \quad (2-12)$$

$$\text{subject to: } 2x_1 + 3x_2 = 0 \quad (2-13)$$

1. First form the Lagrangian Equation:

$$L(x_1, x_2, \lambda) = 4x_1^2 - 3x_2^2 + 2x_1x_2 + 6x_1 - 3x_2 + 5 + \lambda(2x_1 + 3x_2) \quad (2-14)$$

2. Next take the partial derivative with respect to  $x_1$ ,  $x_2$  and  $\lambda$ .

$$\frac{\partial L}{\partial x_1} = 8x_1 + 2x_2 + 6 + 2\lambda \quad (2-15)$$

$$\frac{\partial L}{\partial x_2} = -6x_2 + 2x_1 - 3 + 3\lambda \quad (2-16)$$

$$\frac{\partial L}{\partial \lambda} = 2x_1 + 3x_2 \quad (2-17)$$

3. Solving for our three unknowns:  $x_1 = -3$ ,  $x_2 = 2$  and  $\lambda = 7$ . Our function's minimum value is -7.

Lagrange multipliers have found use in several areas of modern engineering including optimization (discussed in section 2.4) [13] and Finite Element Analysis [14][15]. Lagrange multipliers can be used to augment Castigliano's theorem in order to streamline finding the solution for beam deflection problems[10]. In this application, the constraint equations are the force and moment equilibrium equations.

## 2.3 Dr. Ju's Method

### 2.3.1 Theory

Dr Ju's method requires detailed analysis of the reaction forces at the right side of a beam, as well as, the beam's force and moment equilibrium equations, to determine whether or not the equilibrium equations can be used and included as constraint equations to solve for beam reactions. The procedure works on nearly any beam deflection problem. The procedure is as follows:[10][1]

1. Derive the moment and equilibrium equations for the beam under analysis, solving from left to right. Moments will be summed around the right side of the beam.
2. Determine if the reaction force and moment at the right side of the beam are implicit or explicit in the moment equation. Do they have a volume on which their energy can act? They are explicit if they act through a volume (the location is not at the end of the beam). They are implicit if they act at the end of the beam.

3. Determine if the reaction force and moment are working or non-working. A force is non-working if the deflection is zero. A moment is non-working if the slope is zero at the reaction. Otherwise the force or moment is working.
4. If the reaction is explicit (i.e. present) in the moment equation, its associated equilibrium equation must be included as a constraint for the problem.
5. If the reaction is implicit, then determine if it is working or non-working.
6. Equilibrium equations containing working reactions, regardless of whether or not the reaction is implicit or explicit, must be included as a constraint.

### 2.3.2 Example Problem

The initial problem posed as the analytical model for this thesis consisted of a 42" long shaft supported at four points along its length, with each bearing modeled as a point load. The propeller on the left end of the shaft is modeled as a point load,  $P$ . The weight of the shaft is modeled as a constant distributed load,  $F_s$ , since the shaft is constant diameter and homogeneous in material composition. The right end reactions are modeled as springs, one for the moment and one for the reaction force. The spring model allows different configurations to be modeled; from a free end using a soft spring constant to a cantilever type reaction using a very large spring constant. The free body diagram is below:

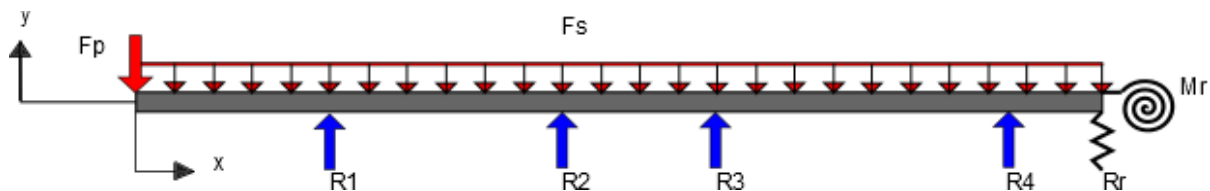


**Figure 12: Free Body Diagram for the Shaft**

Step 1: Using Castigliano's theorem, the moment equation at any point on the shaft is as follows:

$$M(x) = -Px * -\frac{Fsx^2}{2} + R_1(x - x_1) * H_{x_1} + R_2(x - x_2) * H_{x_2} + R_3(x - x_3) * H_{x_3} + R_4(x - x_4) * H_{x_4} \quad (2-18)$$

$P$  = force of the propeller, lbf

$F_s$  = distributed weight of the shaft lbf/in.

$x_{1-4}$  = position of each bearing from the left end of the shaft (in)

$R_{1-4}$  = reaction force at each bearing (lbf)

$H_{x_i}$  is the heavy side step function for  $x_i$  where:

$$H_{x_i} = \begin{cases} 0, & x < x_i \\ 1, & x \geq x_i \end{cases} \quad (2-19)$$

For convenience the following substitution was made:

$$(x - x_1) * H_{x_1} = X_1 \quad (2-20)$$

The moment equation then becomes:

$$M(x) = -Px * -\frac{Fsx^2}{2} + R_1X_1 + R_2X_2 + R_3X_3 + R_4X_4 \quad (2-21)$$

The equilibrium equations are:

$$\sum F_y = -P - FsL + R_1 + R_2 + R_3 + R_4 + R_r = 0 \quad (2-22)$$

$$\sum M_{R_r} = -PL * -\frac{FsL^2}{2} + R_1(L - x_1) + R_2(L - x_2) + R_3(L - x_3) + R_4(L - x_4) + \quad (2-23)$$

$$M_r = 0$$

Step 2: Both  $R_r$  and  $M_r$  are implicit in the equation for  $M(x)$  since neither one acts through a volume of the shaft if the sum of moments is taken about the right side of the shaft. Now we must check to see if they are working or non-working reactions.

Step 3: Both  $R_r$  and  $M_r$  are working since these reactions are modeled as springs and allow the end of the shaft to move under load. Therefore, deflection and slope will not be zero.

Steps 4-6: As a result of our analysis,  $R_r$  and  $M_r$  are implicit –working reactions. According to our decision tree, the since they are both working, both equilibrium equations will be used as to solve for the reactions at each bearing. Now we use the method of Lagrange multipliers to develop our deflection formula.

The deflection formula combines Castigliano's 2<sup>nd</sup> theorem equation with two separate constraint equations. For the deflection at an arbitrary force  $F$ , the deflection equation becomes:

$$\delta_y = \int_0^L \frac{M(x)}{EI} * \frac{\partial M}{\partial F} dx + \lambda_1 * \frac{\partial g_1(x)}{\partial F} + \lambda_2 * \frac{\partial g_2(x)}{\partial F} \quad (2-24)$$

The constraints equations,  $g_1$  and  $g_2$  are listed below (equilibrium equations)

$$g_1 = -P - FsL + R_1 + R_2 + R_3 + R_4 + R_r = 0 \quad (2-25)$$

$$g_2 = -PL * -\frac{FsL^2}{2} + R_1(L - x_1) + R_2(L - x_2) + R_3(L - x_3) \dots \quad (2-26)$$

$$\dots + R_4(L - x_4) + M_r = 0$$

Variation of the moment equation with respect to the five reaction forces, the reaction moment and the two Lagrange multipliers results in a system of 8 equations. These equations can be rearranged into matrix form. This results in a symmetric 8x8 compliance matrix, an 8x1 reaction force vector and an 8x1 deflection vector. These equations were entered into TKSolver and solved using Simpson's rule for numerical integration over 200 steps. The matrices used for calculation purposes in the TKSolver model are shown in Appendix 1.

### 2.3.3 Modeling of the End Reaction/Engine Connection

In the computer model, the engine/shaft connection was modeled as two separate springs. Resistance to vertical movement was modeled as a stiff coil spring while resistance to bending was modeled as a spiral torsional spring.

Derivation of an equation for  $\lambda_1$  began with the use of Hooke's law.

$$R_r = -q_r k_1 \quad (2-27)$$

Therefore

$$q_r = -R_r/k_1 \quad (2-28)$$

Where  $q_r$  is the deflection in inches at the reaction and  $k_1$  is the spring constant for the coil spring (lbf/in). Substitution into the internal energy equation and taking the partial with respect to  $R_r$  yields:

$$-\frac{R_r}{k_1} = \frac{\partial(U + \lambda_1 * g_1(x) + \lambda_2 * g_2(x))}{\partial R_r} \quad (2-29)$$

Results of the variation for each the internal energy term, sum of forces and sum of moments yields:

$$\frac{\partial U}{\partial R_r} = 0 \quad (2-30)$$

$$\frac{\partial g_1}{\partial R_r} = 1 \quad (2-31)$$

$$\frac{\partial g_2}{\partial R_r} = 0 \quad (2-32)$$

Substituting 2-30, 2-31 and 2-32 in to 2-29 and rearranging results in:

$$\lambda_1 = -\frac{R_r}{k_1} \quad (2-33)$$

Dimensional analysis results in units of inches, therefore  $\lambda_1$  is the deflection  $q_r$  at the right reaction  $R_r$ . If the deflection was held to zero at the end (non-working), this term could be ignored.

The same derivation can be made to find  $\lambda_2$ , starting with the equation:

$$M_r = -\theta_r k_2 \quad (2-34)$$

Where  $\theta_r$  is the slope at the right reaction in lb\*in and  $k_2$  is the spring constant for the spiral torsional spring in  $\frac{rad}{lb*in}$ . Substitution in to the internal energy equation and taking the partial with respect to  $M_r$  yields:

$$-\frac{M_r}{k_2} = \frac{\partial(U + \lambda_1 * g_1(x) + \lambda_2 * g_2(x))}{\partial M_r} \quad (2-35)$$

Results of the variation for each the internal energy term, sum of forces and sum of moments yields:

$$\frac{\partial U}{\partial M_r} = 0 \quad (2-36)$$

$$\frac{\partial g_1}{\partial M_r} = 0 \quad (2-37)$$

$$\frac{\partial g_2}{\partial M_r} = 1 \quad (2-38)$$

Substituting 2-36, 2-37 and 2-38 in to 2-35 and rearranging results in:

$$\lambda_2 = -\frac{M_r}{k_2} \quad (2-39)$$

Dimensional analysis results in units of radians, therefore  $\lambda_2$  is the slope at the right reaction  $\theta_r$ . If the slope was held to zero at the end (non-working), this term could be ignored. If both  $\theta_r$  and  $q_r$  are constrained to zero then we have the case of a cantilever beam.

## Chapter 3. Optimization of Bearing Offsets

### 3.1 Introduction to Optimization Theory

#### 3.1.1 Optimization Methods

Two common optimization methods are gradient-based and evolutionary-based methods. Gradient-based search methods use the gradient of an objective function and its constraints to search for an optimum point through an iterative process. In general, this process involves determining a search direction and step size, calculating a new point and checking to determine if this new point is an optimum. If not an optimum, the new point is used as a new starting point and the process is repeated. This method only determines a local optimum, and therefore the final design is heavily dependent on the selection of the initial point. Different starting points may lead to different results[16]. Most gradient based methods require that the objective function be a least twice differentiable. The first derivative is used to determine a gradient for a search direction and the second derivative is used to determine whether or not a local optimum has been found. Also the design variable must be continuous. This means that the design variables must be continuous with-in the allowable design constraints.

Evolutionary based methods do not rely on gradients to determine an optimum point. One of the only requirements is the condition that evaluation of the objective function is possible at any point within the allowable range of the design variables [16]. Evolutionary methods tend to converge at a global optimum; however there is no way to prove mathematically that a global optimum was found.

Evolutionary methods also tend to be computationally expensive. For example, depending on the nature of the problem, the number of design variables, and the degree of convergence, an evolutionary algorithm may require anywhere from five to 200 times as many function evaluations as a gradient-based algorithm. [17] This translates to additional cost in terms of time or number of experiments.

The American Bureau of Shipping (ABS) uses a genetic algorithm, a type of evolutionary method, to determine optimum bearing offsets. [18] A genetic algorithm roughly mimics biological evolution, where the best design is selected after numerous design generations. An initial population is randomly selected consisting of potential designs (design variable

sets) which conform to acceptable design parameters. Each design is assigned a fitness value based on a fitness function. A subset of these designs is randomly selected with a bias toward the most “fit” designs. A new random set of designs is generated based on the previous subset. Since this new set of designs was generated from a subset with higher overall initial fitness, the probability is high that each new generation will have better overall fitness values than the previous generation.[16]

The ABS’s genetic algorithm uses this process to select the 100 best solutions for shaft alignment. Fitness is determined by calculating the smallest standard deviation between bearing loads during different operational conditions. The best or most fit designs have a smaller standard deviation. However, given the detailed nature of the design, a moderate number of design variables and a high degree of convergence, the number of function evaluations might be closer to 200 times more than the number of function evaluations needed for a gradient based solution. While it would be desirable for the purposes of this thesis to achieve such a robust solution, the computational requirements would be beyond most ship based computer systems. A less computationally expensive method is required.

The optimization code written for this thesis used a combination of two gradient based methods; exterior penalty method and steepest descent. These methods will be discussed in detail in Section 3.1.5.

### **3.1.2 Optimization of Bearing Offsets**

Accurately predicting shaft deflection and bearing loads is critical to achieving satisfactory shaft alignment, however this is only the first step. Typically, propulsion shaft alignments are conducted during a dry-dock availability. While this is the easiest time and place to conduct the shaft alignment, the alignment becomes invalid as soon as the ship is placed in the water. While in dry-dock, the weight of the ship is supported by a finite set of blocks along a horizontal plane, but once in the water, the shape of the keel is no longer constrained and the hull sags or hogs depending on the vessel’s current liquid load.

In order to properly align the shaft, data on hull deflections during ballast (no liquid load) and laden (full liquid load) conditions is used to predict an bearing offset arrangement which will maximize the amount of time the ship maintains a satisfactory shaft alignment under any

given operating condition. The tail shaft bearing (aft most bearing) is the baseline 0.0” offset. All other bearings in the system are offset relative to the tail shaft bearing. The goal is to achieve a positive bearing load at each bearing under several normal operating/loading conditions. Each loading condition is weighted based on the operations of the vessel. Crude oil carriers, for example, typically operate at a 50/50 split because they are fully loaded while carrying their cargo to their destination and unloaded during their return trips.

Potentially, an infinite number of solutions exist which may satisfy the above conditions but which is the best solution? The optimum solution depends on the design requirements. For the purposes of this thesis, it was assumed that minimizing the change in the bearing offsets would be the design objective. By minimizing the change in the offsets, cost in terms of redesign or modification of the existing support structure and bearing system can be minimized. The objection function (3-1 below) would therefore minimize the change in the bearing offsets by summing the squares of each offset. The offsets are squared because they can be either positive or negative. The first and often most difficult step in optimization is defining the problem.

### **3.1.3 Standard Optimum Form:**

Defining the problem in Standard Optimum Form helps ensure that all needed information is known and that it is in a format that when solved will minimize the value of the objective function. Standard Optimum Form involves listing all design variables used in the objective function and constraints, listing the objective function and listing all constraints functions. The constraint functions must be rearranged in the form  $g(x) \leq 0$  for inequality constraints and  $h(x) = 0$  for equality constraints. The Standard Optimum Form for the proposed shaft alignment problem is listed below:

Design Variables:  $y_1, y_2, y_3$  (inches)

Vertical Bearing Offsets for the 3 middle bearings.

$$\text{Objective Function: } f(y) = y_1^2 + y_2^2 + y_3^2 \quad (3-1)$$

Since the offsets can be either positive or negative, the sum of the squares of the offsets was minimized.

Subject to: (These are the constraints)

$$g_1(y) : \frac{100 - R_1}{P_y} \leq 0 \quad (3-2)$$

$$g_2(y) : \frac{100 - R_2}{P_y} \leq 0 \quad (3-3)$$

$$g_3(y) : \frac{100 - R_3}{P_y} \leq 0 \quad (3-4)$$

$$g_4(y) : \frac{100 - R_4}{P_y} \leq 0 \quad (3-5)$$

$$g_5(y) : \frac{100 - R_r}{P_y} \leq 0 \quad (3-6)$$

$$g_6(y) : \frac{R_1 - P_y}{P_y} \leq 0 \quad (3-7)$$

$$g_7(y) : \frac{R_2 - P_y}{P_y} \leq 0 \quad (3-8)$$

$$g_8(y) : \frac{R_3 - P_y}{P_y} \leq 0 \quad (3-9)$$

$$g_9(y) : \frac{R_4 - P_y}{P_y} \leq 0 \quad (3-10)$$

$$g_{10}(y) : \frac{R_r - P_y}{P_y} \leq 0 \quad (3-11)$$

$$g_{11}(y) : \frac{\theta - .0003}{.0003} \leq 0 \quad (3-12)$$

$$h_1(y) : -P - Fs + R_1 + R_2 + R_3 + R_4 + R_r = 0 \quad (3-13)$$

$$h_2(y) = -PL - .5FsL^2 + R_1(L - x_1) + R_2(L - x_2) + R_3(L - x_3) + R_4(L - x_4) + Mr = 0 \quad (3-14)$$

-- $R_1, R_2, R_3, R_4, R_r$  are the reactions at each bearing (lbs). These are solved for in TKSolver. The initial bearing offsets are passed from MATLAB to TKSolver and the reactions are passed back to MATLAB.

-- $y_1, y_2, y_3$  are the vertical offsets. These design variables are technically discrete variables since typical shim machining tolerance is .0005". These variables were treated as continuous variables and then rounded to the nearest .0005" and checked to ensure the offsets still satisfied all constraints.

-- $P$  is the Propeller Weight (lbs)

-- $F_s$  is the distributed shaft weight (lbs/in)

-- $L$  is the length of the shaft (in)

-- $x_1, x_2, x_3, x_4$  are the horizontal bearing positions relative to the propeller. (in)

-- $\theta$  is the shaft/bearing misalignment at the tail shaft bearing (rad).

### 3.1.4 Description of Design Variables, Constraints and Objective Functions

Since the TKSolver model allows bearing horizontal locations and vertical offsets, as well as shaft material and size, to be changed in order to test different configurations, it lends itself readily to optimization by providing a wide variety of design variable choices. It returns reactions as well as moments, deflections and slopes at any point on the shaft.

The optimization algorithm needed to move the bearings up and down to achieve positive loading for each bearing. The TKSolver system model only allows the first 4 bearings to be moved. The tail shaft bearing ( $R_1$ ) height remained fixed since it is considered the baseline and the three middle bearings heights were moved to achieve the desired alignment. The engine connection ( $R_r$ ) height dependent upon the modeled spring reaction and is not controlled as the model is currently written. Therefore the design variable set consisted of the 3 middle bearings. The value of the offsets could be either positive or negative. The desired end configuration was a set of bearing offsets which would achieve the below conditions while minimizing the total offsets resulting in the objective function 3-1:

1. All bearing loads must be positive. In other words, the shaft must rest on the bottom of the bearing since this is where strength of the bearing and support structure lie.
2. All bearing loads must be less than 87 lbs/in<sup>2</sup>. This is a requirement set by ABS for composite journal bearing material.

3. The shaft/bearing misalignment angle at the tail shaft bearing must be less than .0003 radians. This requirement is also set by ABS.
4. The sum of forces and moments on the shaft must equal zero.

Constraints: The above conditions result in 11 inequality and 2 equality constraints. Initially the allowable range for the bearing reactions was  $0 \leq R_n \leq 1259 \text{ lbs}$ . This load was derived from condition 2 above, assuming a bearing contact area of 5%. However, since this would result in an offset arrangement where a slight change in hull deflection could result in an unloaded bearing, the minimum bearing load was increased in order to achieve a more stable design. 100 lbs was selected as a realistic minimum bearing load. Increasing the load beyond this point greatly increased the time required for the algorithm to achieve a solution.

The new constraint became:

$$100 \leq R_n \leq 1259 \text{ lbs} \quad (3-15)$$

In order change this into a usable form for the optimization code, the above side-bounded condition on R had to be divided in to 2 separate constraints converted into a standard form. Rearranging the above constrain for the lower bound yielded:

$$100 - R_n \leq 0 \quad (3-16)$$

Normalizing by the maximum load,  $P_y$ :

$$\frac{100 - R_n}{P_y} \leq 0 \quad (3-17)$$

Similarly for the upper bound:

$$R_n \leq 1259 \text{ lbs} \quad (3-18)$$

Became:

$$\frac{R_n - P_y}{P_y} \leq 0 \quad (3-19)$$

The equality constraints are simply the force and moment equilibrium equations. Now that the problem was fully formed it could be applied to an optimization algorithm.

### 3.1.5 Exterior Penalty Method with Steepest Descent Method

The exterior penalty method is a gradient based algorithm which searches through an infeasible design region using a modified Lagrange function. This function penalizes each violated constraint using a constant multiplier which increases in magnitude with each loop.

The modified Lagrange function has the following form: [16]

$$\varphi(y_i, r) = f(y_i) + r * \left[ \sum_{j=1}^m [g_j^+(y)]^2 + \sum_{k=1}^p [h_k(y)]^2 \right] \quad (3-20)$$

$\Phi$  is the descent function

$f(y)$  is the objective function

$g(y)$  are any violated inequality constraints (i.e.  $g > 0$ )

$h(y)$  are any violated equality constraints

$y$  is the vector of design variables

$r$  is the scalar penalty parameter,  $r > 0$

In order to find a search direction, the partial derivative of the descent function  $\phi$  is taken with respect to each design variable. This becomes the vector  $c$ . Note that since  $r$  is a scalar value (usually  $r = 1$  on the first iteration), the partial derivative of the descent function with respect to  $r$ , is zero. This results in an  $i \times 1$  vector.

$$c = \frac{\delta \varphi(y_i, r)}{\delta y_i} \quad (3-21)$$

Now that the gradient vector  $c$  has been calculated, several different methods can be used to determine search direction and distance. In the steepest descent method, the search direction  $d$  is the negative of the gradient vector  $c$ .

$$d = -c \quad (3-22)$$

The search distance is calculated by first evaluating the following expression:

$$y_i^1 = y_i^0 + \alpha * d \quad (3-23)$$

$y_i^1$  is the new point,

$y_i^0$  is the previous point

$\alpha$  is the step size.

Since the previous point and the search direction are known, this forms an  $i \times 1$  vector for each design variable in terms of  $\alpha$ . These expressions are substituted in to the objective function. Next, the partial derivative of the function is taken with respect to  $\alpha$  and all values of  $\alpha$  are solved for. The smallest positive, real value of  $\alpha$  is used for the next search distance. Now that all values needed to calculate the next search point,  $y_i^1$  have been found, the next search point is calculated. This process is repeated a convergence condition is achieved.

Usually when the search distance equals zero we can say that the solution has converged, however  $\alpha$  is a calculated quantity from the search direction, so the search direction is used to determine convergence. The norm of the search direction vector is found at the end of each iteration of the steepest-descent method. Once the norm has reach zero, the algorithm has reached convergence. Usually, a relatively small value close to zero is chosen as a convergence criterion to save time, since the level of accuracy needed in the design can be achieved before the algorithm, reaches zero.

Now that the steepest descent method has converged, the new point is used to check to see if all constraints are satisfied. If so, the search has ended, the exterior penalty method has converged and a solution has been found. If, at the new point, one or more of the constraints

are still violated,  $r$  is increased by a predetermined factor, a new descent function is built and the process is repeated.

### 3.2 Optimization Code Description

The optimization code consisted of a script written in MATLAB. The MATLAB code used nested-while loops, running a steepest descent algorithm within an exterior penalty algorithm. The TKSolver Shaft model was used as a “Black Box” from which to pull data on bearing reactions.

Communication between programs was accomplished by writing a simple visual basic code. This code halted the MATLAB code while it opened TKSolver, ran the deflection program and closed TKSolver. A 3 second pause was inserted after the visual basic code to give TKSolver enough time to close completely, otherwise MATLAB would loop and attempted to open TKSolver again before it had completely closed. This avoided errors generated by empty data sets being returned to MATLAB.

The program begins by developing function approximations from experimental data, in order to reduce the time needed to run the optimization program. This process is discussed in detail in section 3.3. The program then sends the initial point to TKSolver, solves for the bearing reactions and exports the data back to MATLAB.

Once values were obtained using the initial point, the exterior penalty method loop was initiated, and the descent function was built. The gradient of the descent function,  $c$ , and the descent direction vector,  $d$ , were calculated. The step size,  $a$ , was solved for using a symbolic equation solving sub routine. The norm of search direction vector,  $d$ , was checked to see if it was less than the convergence criteria for the loop. If convergence was achieved the program exited to the exterior penalty method loop otherwise the steepest descent loop continued.

The new point was evaluated in TKSolver to determine which constraints were violated. If while building the descent function, all equality and inequality constraints were satisfied so that the norm of the  $g_i$  and  $h_j$  vectors were equal to zero, the problem was considered to have

achieved convergence. If not a new descent function was built from the latest search point data and the exterior penalty loop repeated.

### 3.3 Development of Function Approximations

Developing function approximations was necessary in order to find an approximate relation between the bearing loads and the offsets, so that the optimization program did not have to communicate with the TKSolver model while in the steepest descent loop. The time needed (almost 6 seconds) to run through this subroutine became very expensive after even a few iterations. The steepest descent loop could take 100s or even 1000's of iterations to reach convergence.

Prior to the initial optimization run, linear, quadratic and cubic function approximations were generated using 25 randomly selected design vectors with offset values between -.2" and .2" from the baseline. The design set size was selected so that it would be large enough to accommodate higher level approximation functions if lower level approximations proved to be inaccurate[17]. The initial offset range was selected from the author's previous work experience in checking shaft alignments. A sample function approximation is listed below. This is a cubic form.

$$f(x) = B_0 + B_1y_1 + B_2y_2 + B_3y_3 + B_4y_1^2 + B_5y_2^2 + B_6y_3^2 + B_7y_1^3 + B_8y_2^3 + B_9y_3^3 \quad (3-24)$$

A linear form would truncate the equation after the fourth term. A quadratic approximation would truncate after the 7<sup>th</sup> term. Interaction terms were neglected for two reasons. First, the level of accuracy provided by these terms isn't usually needed until the optimization algorithm is very close to the final optimum point. Second given the discrete nature of the design variables (rounded to the nearest 0.0005"), the level of accuracy gained by using a higher level approximation with interaction terms near the optimum point was needed to obtain a feasible solution.

The  $B$  terms were solved for using:

$$B = R * y^{-1} \quad (3-25)$$

The errors for the linear and cubic approximation functions were nearly equal. The quadratic approximation error was approximately 30% larger at each bearing. The cubic approximation was chosen, since its error was slightly less than the linear approximation error.

The approximation functions were updated each time the optimization program achieved a solution in order to ensure convergence. A new set of 25 experiments were run at random point clustered around the new potential optimum. The optimization program was run again and the new point was compared to the previous optimum. If within the .0005" machining tolerance, convergence had occurred.

**Table 1: Function Approximation Errors**

Bearing	Linear	% Linear diff	Quadratic	% Quad diff	Cubic
R_1	0.231516738	1.82%	0.294788059	29.65%	0.227376
R_2	1.615673234	2.15%	2.055456154	29.96%	1.581645
R_3	3.583713158	2.20%	4.558936279	30.01%	3.506708
R_4	4.012792045	2.21%	5.104713508	30.02%	3.926003
R_R	1.813063705	2.22%	2.306382449	30.03%	1.773697

### 3.4 Results

The initial design variable vector was [0 0 0]. This point was selected since it violated the design requirements. This resulted in bearing reactions of:

**Table 2: Initial Bearing Reactions**

Bearing	Load	Unit	Comment
R_1	515.0938547	lbs	
R_2	448.9524798	lbs	
R_3	414.5085502	lbs	
R_4	-61.64931395	lbs	
R_R	105.3883373	lbs	reaction at engine coupling (lbs)

Constraint 4 was violated since the bearing reaction was negative.

The final design variable vector was [0.0026", -0.0123", -0.0019"]. These offsets were checked in TKSolver and resulted in bearing reactions of:

**Table 3: Final Bearing Reactions (non-discrete offsets)**

Bearing	Load	Unit	Comment
R_1	502.4115313	lbs	
R_2	500.6624283	lbs	
R_3	220.1501782	lbs	
R_4	95.73257297	lbs	
R_R	103.3371973	lbs	reaction at engine coupling (lbs)

The results indicated that constraint 4 was violated and constraint 5 was active. The violated constraint is a result of a slight relaxation of the  $\leq 0$  requirement in the MATLAB exterior penalty code and error in the function approximation.

Since shim machining tolerance is only accurate to within 0.0005", the following vectors were investigated to check for the most desirable solution:

[0.0025", -0.012", -0.002"]

[0.0025", -0.0125", -0.002"]

[0.0025", -0.013", -0.002"]

The third option resulted in the best results with all constraints satisfied and only constraints 4 and 5 active.

**Table 4: Final Bearing Reactions (Discrete Offsets)**

Bearing	Load	Unit	Comment
R_1	501.8880811	lbs	
R_2	503.0612704	lbs	
R_3	209.7187262	lbs	
R_4	105.9442426	lbs	
R_R	101.6815878	lbs	reaction at engine coupling (lbs)

The final objection function value was  $0.0001617 \text{ in}^2$ . Using discrete values the objective function value increased to  $0.0001792 \text{ in}^2$ .

The results of the first function approximation yielded a final point of  $[0.0027'', -0.0129'', -0.0020'']$ . To refine this point and verify convergence, experiments were run on 25 new points near this result and the code was run again using the new function approximations. The second iteration resulted in a new point  $[0.0026'', -0.0123'', -0.0019'']$ . The change vector  $[-0.0001'', 0.0006'', 0.0001'']$  was relatively small; however the change in the middle offset was less than feasible the machining tolerances. At this point, discrete design vectors were investigated in order to select the most desirable results. It was more efficient to run 3 more experiments rather than selecting 25 additional points in order to improve the function approximation. The first and third offsets were rounded to the closest  $0.0005''$  and experiments were run at  $-0.012$ ,  $-0.0125$  and  $-0.013''$  for the R3 bearing offset.

### 3.5 Conclusions

The optimization program found a valid set of offsets which met all of the design requirements and ABS standards within two function approximation iterations.

The offsets were within the expected range of the initial experimental points used to develop the function approximation. At full scale, the weight of the shaft dominates the deflections seen in the shaft, which explains why the 3<sup>rd</sup> bearing had to be lowered significantly in order to remove the negative reaction in the 4<sup>th</sup> bearing.

Optimization of the system may prove difficult for the Laden and Ballast conditions. The shaft system model is very unstable, with the 3<sup>rd</sup> and 4<sup>th</sup> bearing loads varying greatly with extremely minor changes in bearing heights. This is reflexed in the function approximation error since the magnitude of the errors is much higher at the 3<sup>rd</sup> and 4<sup>th</sup> bearing. The current TK model uses springs to approximate the engine to shaft interface at bearing 5. The spring constants are set high to create a near cantilever condition. A load representing the bull gear at this connection may make the loads more stable.

## Chapter 4. Methodology and Data Collection

### 4.1 Overview

This chapter documents the methodology, data collection, and initial data analysis.

### 4.2 Methodology

#### 4.2.1 Model System

The system built for experimental verification of the analytical model is modeled after a 110' Island Class Patrol boat which is currently used by the U. S. Coast Guard. This propulsion system consists of two propulsion diesel engines each independently coupled to its own reduction gear, shaft and propeller. Each shaft is 28' long by 4" in diameter and is made of K500 Monel. Each end of the shaft is tapered to fit to the propeller and bull gear. The shaft is one piece.

K500 Monel is commonly used in marine environments because of its superb anticorrosive properties and high strength. K500 is a nickel-copper (63%/33%) alloy which is precipitation hardened with aluminum (3.15%) and titanium (0.85%). Its modulus of elasticity is 179,000 kPa. Due to Monel's high price and no available funding for research, several substitute materials were used including a C110 copper rectangular bar, a 1018 steel rod and a 4130 steel tube.

#### 4.2.2 Scaling of the Propulsion System

The original intent was to make a 1/8 scale model of the actual system and test it experimentally against the computer model. After the computer model was validated a full sized system would be tested. However, several scaling issues made this impractical. The moment of inertia for the 1/8 scale shaft was 4096 ( $8^4$ ) times smaller than the moment of inertia of the actual system. Also the shaft's distributed weight for the scale model was 64 ( $8^2$ ) times smaller than the actual distributed weight of the shaft. These differences naturally resulted in completely different deflection results (shown below).

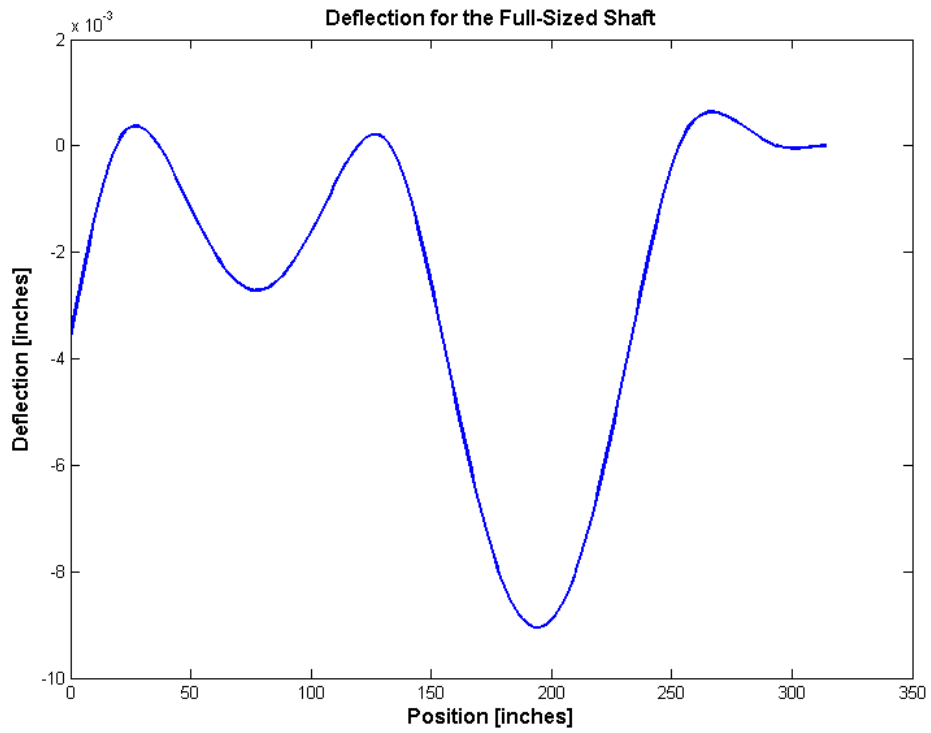


**Figure 13: Full Scale Deflection Results**

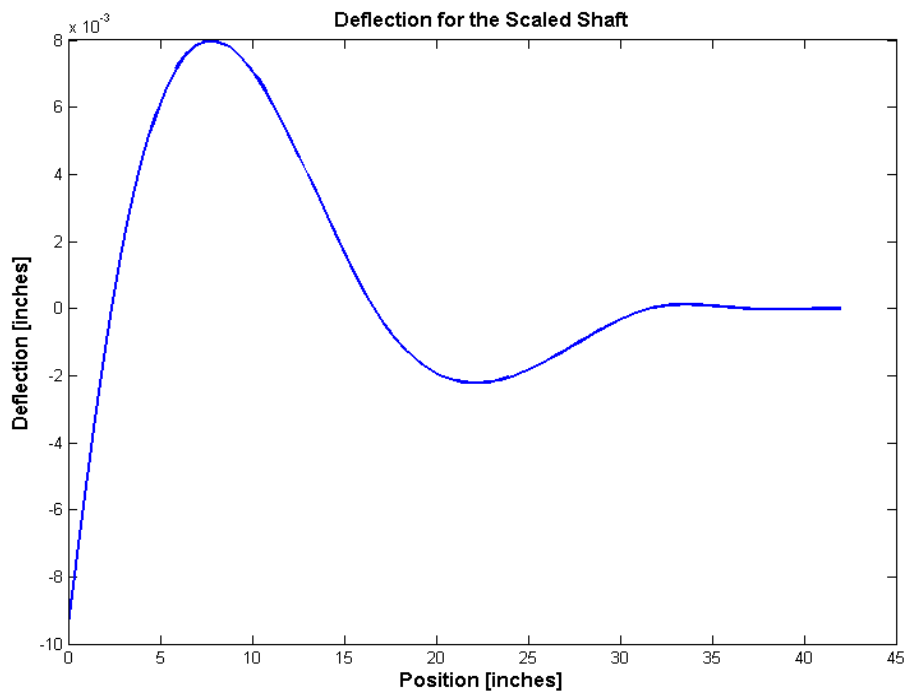


**Figure 14: Scaled (1/8) Deflection Results**

Since scaling proved to be impractical and gathering experimental data from an actual ship was infeasible due to lack of funding and travel time (the closest ships were home ported in Port Angeles, WA or Coos Bay, OR), numerous departures from the actual ship configuration were made to facilitate experimental validation of the model. Since the intent of the experimental rig was to test the accuracy of the model, the only critical test configuration criteria was that experimental model could be accurately reproduced in the computer model.

### 4.2.3 Experimental Model Fabrication

An old Bridgeport Mill base was used as a stable test platform on which to mount the shaft. It was rigid enough not to measurably deflect when the shaft was loaded during testing. This approximates the desired design condition for large vessels where the hull structure is stiffer than the propulsion shaft. Prior to testing, the mill base was leveled using the four leveling screws on the rolling base.



**Figure 15: An Old Bridgeport Mill Base was used as the Experiment Test Bed**

The first experiment used a 0.5" OD 4130 mild steel tube (0.399" ID). The small moment of inertia for the tube allowed for relatively large deflections and more easily measurable and verifiable results. The bearings were reduced in scale length from 2" to 1" both for ease of machining and to allow the shaft to deflect more under load. The shaft length was scaled to 1":8" to match the length of the test platform. The overall scaled shaft length was 42". The bearings were machined from solid blocks of 6061-T6 aluminum. They were bolted to the

test bed using 3/8" bolts designed for mounting fixtures to the mill. Each bearing was reamed to 0.505" ID.



**Figure 16: Initial Modeled Engine End Connection**

Initially the engine connection was modeled using a simple clamp shown in Figure 16. This proved impractical since in order to prevent longitudinal movement of the shaft, the clamp had to be tightened down significantly. This imparted a large load the end of the shaft which in turn caused significant deflection.

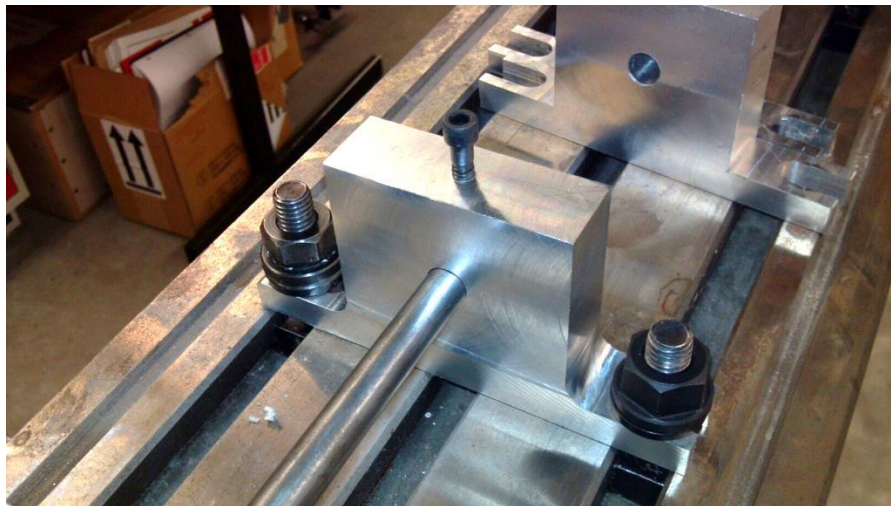


**Figure 17: Final Engine End Connection Model**

To correct this deficiency, a fifth bearing was machined to model the end connection. A hole for a 1/4-20 set-screw was machined into the top center of the bearing to hold the shaft in place without imparting a significant deflection on the shaft.



**Figure 18: First Experimental Set up (steel tube)**

#### **4.2.4 Test Configurations**

The first test configuration used 2 bearings and the engine end connection. The front of the first bearing was positioned at 16” from the weighted end of the shaft. The front of the second bearing was positioned 36” from weighted end of the shaft. These bearing positions allowed for a relatively large deflection at any point on the shaft once weight was applied. Deflection was measured at 6 locations along the shaft and compared to the computer model predictions. In the computer model, bearings were placed at 16”, 17”, 36” and 37” to model the contact points at either end of the actual bearings. The effective offset of each bearing face was measured by recording the distance to the bottom of the shaft from the test bed, both at the front and back of the bearing. The offset reflected the allowable movement of the shaft due to the difference between the OD of the shaft and the ID of the bearing. The offsets at

17" and 36" were 0.0035". The offset at 37" was 0.001". Because the computer-modeled bearing at 16" is considered the baseline, its offset was set to 0".

The second test configuration was identical to the first except a 0.5" OD solid 4130 steel rod was tested. The weights were suspended from the end of the shaft by small gauge wire. A solid shaft was selected to attempt to resolve the relatively large difference in predicted and actual results seen at the 5<sup>th</sup> and 6<sup>th</sup> measurement location. Run-out readings on the 1018 steel tube showed a slight bend in the shaft so a straighter shaft was used to see if the bend affected the results.

The final test configuration was constructed to better represent the point load bearings in the computer model. The boundary conditions at each bearing could be more closely approximated at each bearing. A 1" by 3/8" C110 copper bar was used as a shaft. A rectangular shaft was selected to eliminate possible pre-stressing during machining. The bearings were positioned at 17.25", 21.75", 38.75" and 42.75" from the weighted end of the shaft. The large gap in the middle of the shaft allowed for a measurable deflection. Weights were hung from the end of the shaft by a small gauge wire.

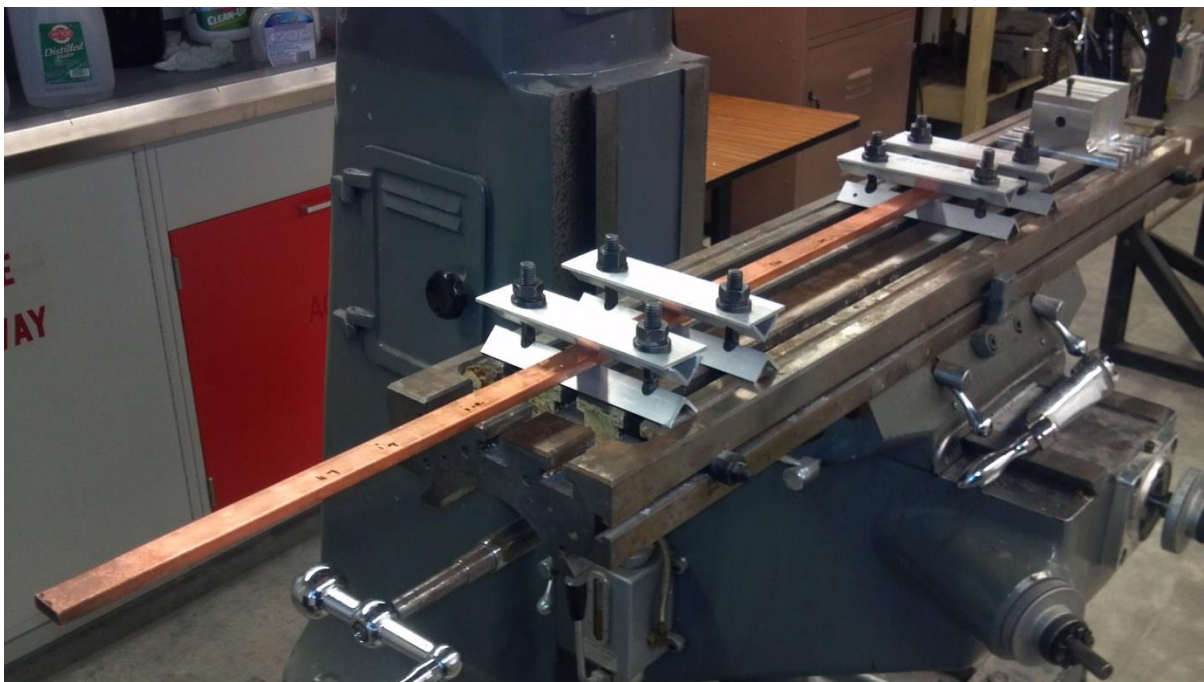


**Figure 19: Configuration for Rectangular Bar Test**



**Figure 20: Point Load Bearing**

### **4.3 Deflection Measurement**

#### **4.3.1 Experimental Procedure**

The actual shaft deflection was measured using a dial indicator. The maximum resolution of the dial indicator gage was 0.001". The 0.0001" digit in the data was estimated by eye. Deflection measurements for the first 2 configurations were taken at 6 locations from the weighted end of the shaft: 7" (the farthest point the dial indicator could reach from the test bed), 9", 12", 21", 24" and 27". The deflection readings for the final configuration, shown in Figures 20 & 21, were measured at 7", 9", 12", 24", 27" and 30". Deflection readings were taken at no load, 2.205 lbs and 4.41 lbs. The spring force applied by the dial indicator was neglected.

#### **4.3.2 Computer Model Data Preparation**

The computer calculations needed to be adjusted before results could be compared. Since the shaft deflects under its own weight, this deflection had to be subtracted from the computer results before it could be compared to the experimental data. Also, since the measurement locations on the shaft did not coincide directly with the calculated data points in the computer model, results had to be interpolated between data points. The shaft was divided into 200

equal sections of 0.21375". Since shaft deflection was small and the distance between points was small, linear interpolation was used to solve for deflection at each of the six measurement points.

## 4.4 Data Collection

### 4.4.1 Experimental Error

Overall, experimental results were consistent between experimental models and matched closely with the computer model predictions. The percent error listed in the following tables references the percent error in the model deflection ( $\delta_{model}$ ) when compared to the experimental results ( $\delta_{experiment}$ ).

$$error = \frac{(\delta_{model} - \delta_{experiment})}{\delta_{experiment}} \quad (4-1)$$

Error in the model's results can be attributed to several factors. In the pipe and tube configurations, there was uncertainty in the boundary conditions at each bearing. Accurately measuring the vertical offset for each bearing proved difficult.

Two limitations in the design of the computer model made it difficult to compensate for the uncertainty in the boundary conditions at the bearings. First, the number of bearings in the model was fixed at four. This could be partially overcome by pairing and spacing bearings extremely close together to create essentially one bearing. This would model the boundary conditions at the entrance and exit of a single bearing. However, spacing the model bearings less than 1" apart made it impossible to measure the actual offset of the shaft from the bearing. This leads into the second limitation. The shaft's deflection is constrained to the offset entered at each bearing. This creates an unrealistic constraint where the shaft must remain in contact with the bottom of bearing surface. The deflection results were extremely sensitive to the bearing offsets so that a small error would lead to large differences in the predicted deflection curve for the shaft. In the experiment, the shaft was free to pivot inside the bearing within the 0.005" difference between the OD of the tube and the ID of the bearing.

Some simplifying assumptions lead to error in the final prediction of the deflection curves. The bearings and the shaft contact points were considered rigid. The model doesn't take into

account either bending of the bearings or local deformation of the shaft at the point of contact with the bearing. Finally, the actual modulus of elasticity for the shaft isn't known.

## 4.4.2 Experimental Results

### 4.4.2.1 4130 Steel Tube

The initial experimental measurements were taken on a 4130 steel tube. Results for the 2.205 lbs weight were consistent with the error between the 2 models ranged from 9 to 18%. Although the range in error between readings appears much larger for the interior readings, these deflections are much smaller and are much more susceptible to measurement errors.

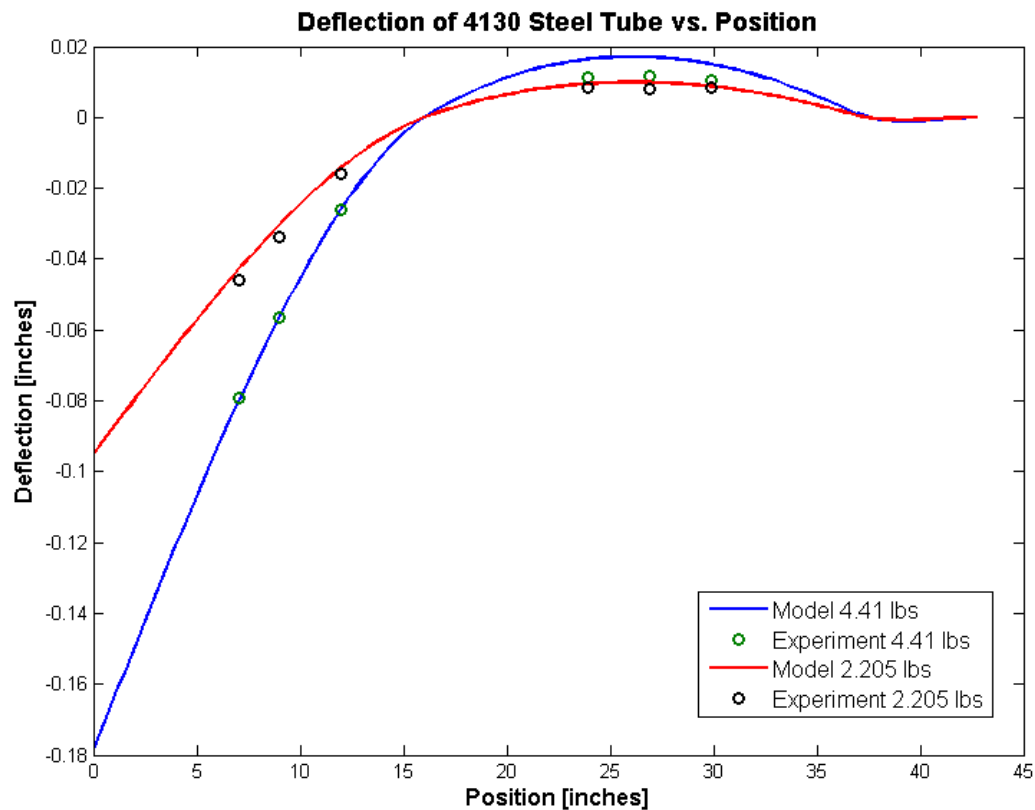


**Figure 21: Plot of 4130 Steel Tube Experimental and Model Deflections**

**Table 5: Results for the 4130 Steel Tube (2.205 lbs)**

Position (in)	Model (in)	Experiment (in)	% Difference	Calculated Difference (in)
7	-0.0418	-0.046	-9.24%	-0.0042
9	-0.0294	-0.0338	-12.95%	-0.0044
12	-0.0138	-0.016	-13.85%	-0.0022
21	0.0076	0.0085	-10.79%	0.0009
24	0.0097	0.0082	17.73%	-0.0015
27	0.01	0.0085	17.95%	-0.0015

For the 4.41 lbs weight results, the first three measurement locations (7", 9" and 12") were within approximately 2% of the actual measurements. However, the error dramatically increased when measurements were taken between bearings. Several more experiments were run to verify the accuracy of the initial results and refine experimental techniques. Table 6 summarizes the final results 4.41 lbs weight.

**Table 6: Results for the 4130 Steel Tube (4.41 lbs)**

Position (in)	Model (in)	Experiment (in)	% Difference	Calculated Difference (in)
7	-0.0789	-0.079	-0.09%	-0.0001
9	-0.0553	-0.0565	-2.12%	-0.0012
12	-0.0256	-0.026	-1.68%	-0.0004
21	0.0131	0.0113	16.07%	-0.0018
24	0.0166	0.0115	44.37%	-0.0051
27	0.0172	0.0103	66.54%	-0.0069

This error can be attributed to uncertainty in the bearing offsets present at the previous bearing exit and next bearing entrance as well as the relatively small deflection exposing the limitation in the dial indicator's precision. A run out was conducted on the shaft and a perceptible bend was found in the shaft. At 90 degrees rotation counter clockwise, the shaft deflected 0.0257" downward, at 180 degrees; the shaft deflected 0.0127" downward. At 270 degrees it deflected only 0.0035" downward. Figure 22 summarizes these results. Given the results of the run and the fact that there was a high probability that the modulus of elasticity could have been affected by working of the steel into a tube, a solid steel rod was tested.

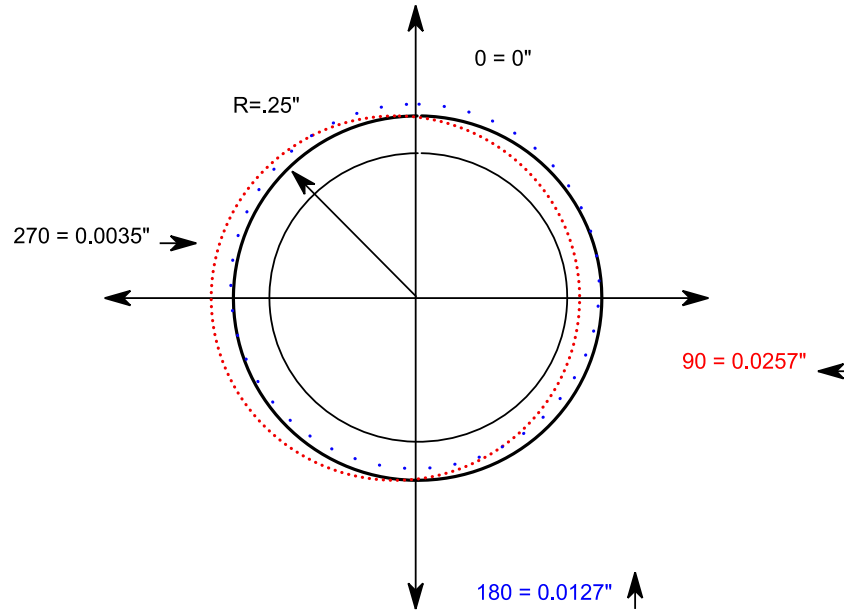


**Figure 22: Shaft Run-out for 4130 Steel Tube**

#### 4.4.2.2 1018 Steel Rod

The second test configuration used a 1018 steel rod. The outside diameter of the rod was 0.5". The rest of the configuration remained unchanged. A run out of the shaft was conducted to check for straightness. Deflection in the 0-180 direction changed by only 0.0008" while deflection in the 90-270 direction changed by only 0.008".

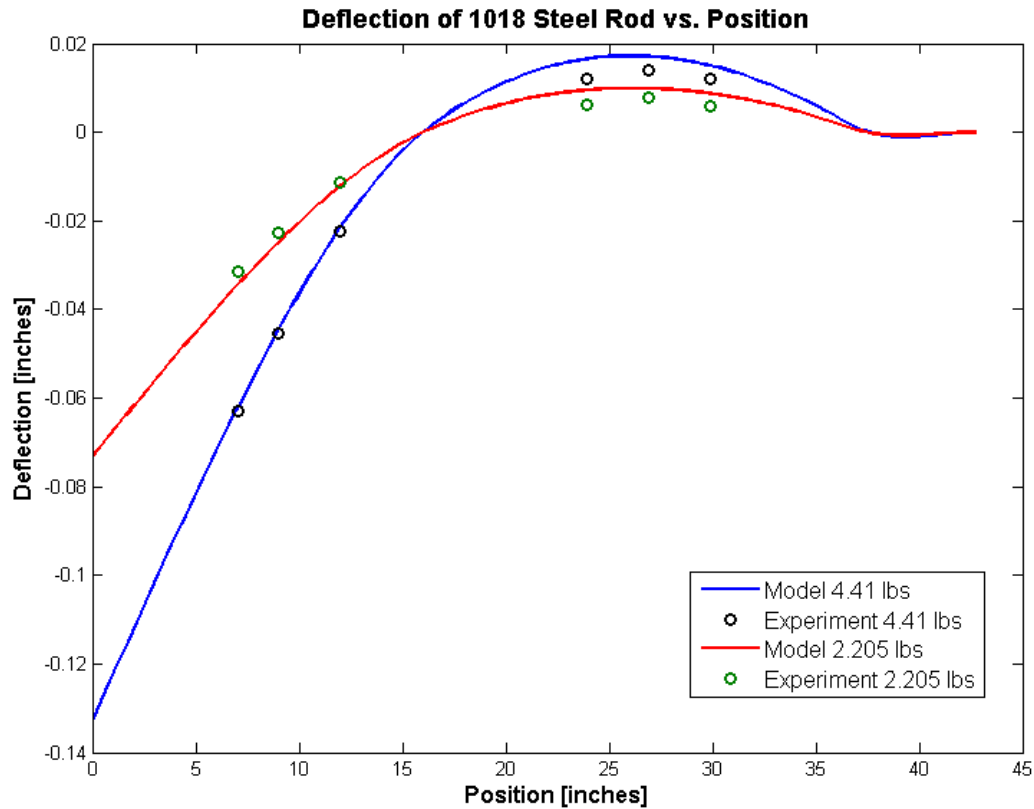


**Figure 23: Plot of 1018 Steel Rod Model and Experimental Deflections**

Results for the 2.205 lbs weight were extremely good until the 27" measurement. This may indicate an error in the offset at the entrance of the 2<sup>nd</sup> bearing.

**Table 7: Results for the 1018 Steel Rod (2.205 lbs)**

Position (in)	Model (in)	Experiment (in)	% Difference	Calculated Difference (in)
7	-0.0298	-0.0315	-5.54%	-0.0017
9	-0.0212	-0.0228	-7.21%	-0.0016
12	-0.0103	-0.0113	-8.86%	-0.001
21	0.0065	0.0063	2.52%	-0.0002
24	0.0082	0.0077	5.85%	-0.0005
27	0.0084	0.006	39.73%	-0.0024

Results for the 4.41 lbs weight were very good through the first four measurements. Again, an error in the measurement of the offset at the entrance of the second bearing may account for the error in the second 2 readings.

**Table 8: Results for the 1018 Steel Rod (4.41 lbs)**

<b>Position (in)</b>	<b>Model (in)</b>	<b>Experiment (in)</b>	<b>% Difference</b>	<b>Calculated Difference (in)</b>
7	-0.0604	-0.063	-4.08%	-0.0026
9	-0.043	-0.0454	-5.24%	-0.0024
12	-0.021	-0.0223	-5.81%	-0.0013
21	0.0133	0.0121	10.16%	-0.0012
24	0.0168	0.014	20.31%	-0.0028
27	0.0173	0.0122	42.20%	-0.0051

#### **4.4.2.3 Copper Bar**

In order to remove the uncertainty in the boundary conditions at the bearings, a new experimental set up was designed to approximate point loads. This configuration was discussed in detail in section 4.2.4 and shown in figures 19 and 20. The measurement locations for the first three bearings remained the same as the other two configurations (7", 9", and 12"). However, due to the location and size of the new bearings the last three locations were shifted by 3" to 24", 27" and 30". The bearings were spaced as far apart as possible in order to maximize deflection at the interior measurements. There were no measurable differences in bearing offsets so the model offsets were set to zero.

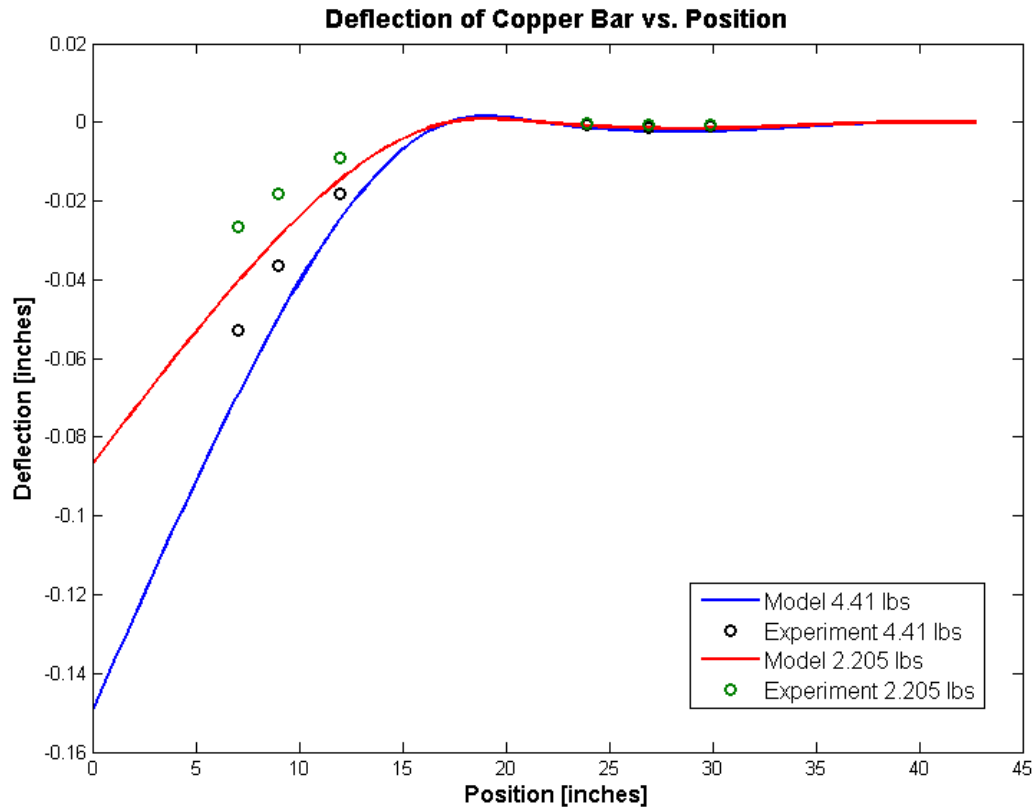


**Figure 24: Plot of C110 Copper Bar Model and Experimental Deflections**

Results for the copper bar were consistent between the two weights. The large error in the interior measurements is due to the small deflection and the limitation in accuracy of the dial indicator. Predicted and actual deflections at the interior readings were three times smaller than the deflections predicted for the first two configurations.

**Table 9: Results for the Copper Bar (2.205 lbs)**

Position (in)	Model (in)	Experiment (in)	% Difference	Calculated Difference (in)
7	-0.0288	-0.0266	8.23%	0.0022
9	-0.0205	-0.018	13.72%	0.0025
12	-0.0101	-0.0092	9.38%	0.0009
24	-0.0005	-0.0003	63.84%	0.0002
27	-0.0007	-0.0006	24.63%	0.0001
30	-0.0007	-0.0005	36.26%	0.0002

**Table 10: Results for the Copper Bar (4.41 lbs)**

<b>Position (in)</b>	<b>Model (in)</b>	<b>Experiment (in)</b>	<b>% Difference</b>	<b>Calculated Difference (in)</b>
7	-0.0576	-0.053	8.64%	0.0046
9	-0.0409	-0.0365	12.16%	0.0044
12	-0.0201	-0.0181	11.20%	0.002
24	-0.001	-0.0008	22.88%	0.0002
27	-0.0015	-0.0013	15.05%	0.0002
30	-0.0014	-0.001	36.26%	0.0004

## **Chapter 5. Conclusions and Recommendations**

### **5.1 Conclusions**

Dr. Ju's method proved a sound basis for a simple computer model for beam deflection. The experimental data validated the model results in all three configurations. Results were very accurate when the influence of the boundary conditions at the bearings could be minimized. This was especially clear in measurements taken prior to the first bearing where the offset was zero in all cases where the offset was not influenced by the loading at the end of the shaft or the spacing of the bearings.

### **5.2 Future Work and Recommendations**

By trial and error a nearly exact solution could be found for the measured deflections, Since the deflection curve was highly influenced by the bearing offsets. In future work, the optimization program discussed in chapter 3 could be modified to search for the offsets which would match the measured results, to achieve a very accurate picture of the shaft's alignment. This would be especially useful in situations where the offsets could not be measured directly.

Use of the original end connection model shown in Figure 16 could be used to model different working reactions to further investigate Dr. Ju's methods. The end of the shaft can be deflected easily and the displacement measured to create a sizable working reaction. The TKSolver model would need to be modified to accept a constrained end deflection. In its current state as it solves for both the moment and reaction forces.

Other future work could include adding the influence of the hull's deflection under different conditions. Also the bearings can be changed to represent a distributed load and the offset restrictions could become condition based on whether or not the shaft deflection is restricted by the bearing's dimensions.

## References

- [1] Ju, F. D., "On the Constraints for Castigliano's Theorem," *Journal Frankl. Inst.*, vol. 292, no. 4, pp. 257–264, Oct. 1971.
- [2] *RULES FOR BUILDING AND CLASSING STEEL VESSELS 2014*. ABS Plaza 16855 Northchase Drive Houston, TX 77060 USA: American Bureau of Shipping Incorporated by Act of Legislature of the State of New York 1862, 2013.
- [3] *ABS GUIDANCE NOTES ON PROPULSION SHAFTING ALIGNMENT*. American Bureau of Shipping ABS Plaza 16855 Northchase Drive Houston, TX 77060 USA: American Bureau of Shipping, 2006.
- [4] C. B. Barrass, *Ship design and performance for masters and mates*. Oxford: Elsevier Butterworth-Heinemann, 2004.
- [5] V. Bertram, *Practical Ship Hydrodynamics*. Butterworth-Heinemann, 2000.
- [6] D. Woodyard, *Pounder's Marine Diesel Engines and Gas Turbines*. Butterworth-Heinemann, 2009.
- [7] E. F. Northrup, *Methods of Measuring Electrical Resistance*. McGraw-Hill book Company, 1912.
- [8] I.-C. Jong and J. Rencis, "ANALYSIS OF STATICALLY INDETERMINATE REACTIONS AND DEFLECTIONS OF BEAMS USING MODEL FORMULAS: A NEW APPROACH," *Am. Soc. Eng. Educ. 2007*, vol. AC 2007–11, 2007.
- [9] J. Rencis and H. Grandin T., "Solving Beam Deflection Problems using a Tradition Approach," *Proc. 2009 Midwest Sect. Conf. Am. Soc. Eng. Educ.*, p. 21, 2009.
- [10] F. D. Ju, "Generalized Castigliano's Principal." Mechanical Engineering Dept. University of New Mexico.
- [11] A. P. Boresi and R. J. Schmidt, *Advanced mechanics of materials*. New York: John Wiley & Sons, 2003.

- [12] J. L. Lagrange, A. C. Boissonnade, and V. N. Vagliente, *Analytical mechanics*. Dordrecht; Boston, Mass.: Kluwer Academic Publishers, 1997.
- [13] A. S. Kucuk Ismail, "Optimal Design of a Beam under Uncertain Loads," *Lect. Notes Eng. Comput. Sci.*, 2009.
- [14] J. N. Reddy, *An Introduction to the Finite Element Method, 3rd Edition (McGraw Hill Series in Mechanical Engineering)*. McGraw Hill India.
- [15] O. C. Zienkiewicz, R. L. Taylor, and J. Z. Zhu, *The Finite Element Method: Its Basis and Fundamentals, Sixth Edition*, 6 edition. Butterworth-Heinemann, 2005.
- [16] J. Arora, *Introduction to Optimum Design*. [s.l.: Elsevier textbooks, 2011.
- [17] D. W. Zingg, M. Nemeč, and T. H. Pulliam, "A comparative evaluation of genetic and gradient-based algorithms applied to aerodynamic optimization," *REM N*, vol. 17/2008, pp. 103–126.
- [18] D. Sverko, "A Solution to Robust Shaft Alignment Design," *PropellersShafting Symp. Va. Beach- Sept. 12-13 2006*.

## **Appendix A: TKSolver Shaft Deflection Code**

This Appendix Shows the TKSolver used to solve the beam deflection problem. The Rule Sheet is shown first followed by each function in the order they are called out in the rule sheet.

Rule	
$I = \pi \cdot (d_o^4 - d_i^4) / 64;$	moment of inertia
$EI = E \cdot I;$	flexural modulus
$F_s = \rho \cdot \pi \cdot ((d_o/2)^2 - (d_i/2)^2) / (12^3)$	
$k_2 = \text{Scale}_2 \cdot EI$	
$k_1 = \text{Scale}_1 \cdot EI;$	spring constant for engine coupler
call precalc();	calculates the matrix "a" and the column vector "b"
call \$LINSOLVE('a','b','sol');	solves for the reaction column vector
call reactions(;R_1,R_2,R_3,R_4, $\lambda_2$ ,M_R, $\lambda_1$ ,R_R);	retrieves the reactions from the "sol" column vector
call displayresults();	calculates the moment and deflection along the beam for plotting
$\Delta P = P + F_s \cdot L - R_1 - R_2 - R_3 - R_4 - R_R$	
$\Delta M = P \cdot L + .5 \cdot F_s \cdot L^2 - R_1 \cdot (L - x_1) - R_2 \cdot (L - x_2) - R_3 \cdot (L - x_3) - R_4 \cdot (L - x_4) - M_R$	

#### Precalc Function:

The Simpson function is a built in TKSolver Function found in the Application/TKSolver 5 Library/Mathematics/Differentiation and Integration folder.

Statement
'a1[1]=Simpson('Int11,0,L,n)
'a1[2]=Simpson('Int12,0,L,n)
'a1[3]=Simpson('Int13,0,L,n)
'a1[4]=Simpson('Int14,0,L,n)
'a1[5]=L-x_1
'a1[6]=0
'a1[7]=1
'a1[8]=0
'a2[1]='a1[2]
'a2[2]=Simpson('Int22,0,L,n)
'a2[3]=Simpson('Int23,0,L,n)
'a2[4]=Simpson('Int24,0,L,n)
'a2[5]=L-x_2

'a2[6]=0
'a2[7]=1
'a2[8]=0
'a3[1]='a1[3]
'a3[2]='a2[3]
'a3[3]=Simpson('Int33,0,L,n)
'a3[4]=Simpson('Int34,0,L,n)
'a3[5]=L-x_3
'a3[6]=0
'a3[7]=1
'a3[8]=0
'a4[1]='a1[4]
'a4[2]='a2[4]
'a4[3]='a3[4]
'a4[4]=Simpson('Int44,0,L,n)
'a4[5]=L-x_4
'a4[6]=0
'a4[7]=1
'a4[8]=0
'a5[1]='a1[5]
'a5[2]='a2[5]
'a5[3]='a3[5]
'a5[4]='a4[5]
'a5[5]=0
'a5[6]=1
'a5[7]=0
'a5[8]=0
'a6[1]='a1[6]
'a6[2]='a2[6]
'a6[3]='a3[6]
'a6[4]='a4[6]
'a6[5]='a5[6]
'a6[6]=-1/k2

'a6[7]=0
'a6[8]=0
'a7[1]='a1[7]
'a7[2]='a2[7]
'a7[3]='a3[7]
'a7[4]='a4[7]
'a7[5]='a5[7]
'a7[6]='a6[7]
'a7[7]=0
'a7[8]=1
'a8[1]='a1[8]
'a8[2]='a2[8]
'a8[3]='a3[8]
'a8[4]='a4[8]
'a8[5]='a5[8]
'a8[6]='a6[8]
'a8[7]='a7[8]
'a8[8]=-1/k1
'b[1]= $\delta_1 + \text{Simpson}('b1\text{Int}, 0, L, n)$
'b[2]= $\delta_2 + \text{Simpson}('b2\text{Int}, 0, L, n)$
'b[3]= $\delta_3 + \text{Simpson}('b3\text{Int}, 0, L, n)$
'b[4]= $\delta_4 + \text{Simpson}('b4\text{Int}, 0, L, n)$
'b[5]= $P*L + .5*Fs*L^2$
'b[6]=0
'b[7]= $P + Fs*L$
'b[8]=0

### Reactions Function

Statement	
R_1='sol[1];	Reaction at bearing 1
R_2='sol[2];	Reaction at bearing 2
R_3='sol[3];	Reaction at bearing 3
R_4='sol[4];	Reaction at bearing 4
λ2='sol[5];	LaGrange Multiplier
M_R='sol[6];	Moment from weight of bull gear
λ1='sol[7];	deflection at right end
R_R='sol[8];	Reaction at right end

### Display Results Function

Statement	
for i=1 to n+1	
ξ=(i-1)*(L)/n;	beam into n increments
'ξ[i]=ξ;	list of ξ for the x-axis
'ξ1]=ξ;	creates a parameter than can be passes into the numerical integration
'Mx[i]=Mx(ξ)	
'δnum[i]=-(Simpson('Defl,0,L,n)- λ2 (L-ξ)- λ1	
'Mnum[i]=-(Simpson('Moment,0,L,n)-λ2	
next i	

### Mx Function

$z = -P*x - .5*F_s*x^2 + R_1*X_1(x) + R_2*X_2(x) + R_3*X_3(x) + R_4*X_4(x)$ ; This is the moment equation for the shaft.

### DEFL Function

Statement	
ξ= 'ξi[1]	
z=Mx(x)/EI*(-(x-ξ)*H(x,ξ))	

## **Appendix B: MATLAB Optimization Code**

## First Iteration Code

```

clear all
clc
tic

%Parameters
x1=19;
x2=133;
x3=253;
x4=294;
P=220; %Propellor Load (lbs)
Fs=3.82896;
L=314; %Length of beam 2 (inches)
E=26000000; %Modulus of Elasticity (psi)
sigma=87;
percent_contact=5;
contact_area=pi()*5*18*percent_contact/100;
Py=sigma*contact_area; %Yield Strength (psi)
safety_factor=1.5;
num_var=3; % # of design variables
bearing_var=5;
g_eq=10; % # of inequality constraints
h_eq=0; % # of equality constraints
eps_h=.01; % Tolerance for Equality Constraints
eps_g=.001; % Tolerance for Inequality Constraints
eps_SD=.001; % Convergence Criteria
r_val(1)=1; % Initial Penalty Value
r_mult=10; % Penalty Multiplier

x=[1 1 1 1 1 1 1 1 1 1 1 1 1 1 1 1 1
1 1 1 1 1 1 1
0 0.1 -0.1 0 0 0 0 0.1 -0.1 0.2 0 0 -0.2 0 0
0.1 0 0.1 -0.1 0 -0.1 0.2 0.2 0.2 -0.2
0 0 0 0.1 -0.1 0 0 0.1 -0.1 0 0.2 0 0 -0.2 0
0.1 0.1 0 -0.1 -0.1 0 0 -0.2 0.2 -0.2
0 0 0 0 0 0.1 -0.1 0.1 -0.1 0 0 0.2 0 0 -0.2
0 0.1 0.1 0 -0.1 -0.1 -0.2 0 0.2 -0.2
0 0.01 0.01 0 0 0 0 0.01 0.01 0.04 0 0
0.04 0 0 0.01 0 0.01 0.01 0 0.01 0.04 0.04
0.04 0.04
0 0 0 0.01 0.01 0 0 0.01 0.01 0 0.04 0 0
0.04 0 0.01 0.01 0 0.01 0.01 0 0 0.04 0.04
0.04
0 0 0 0 0 0.01 0.01 0.01 0.01 0 0 0.04 0
0 0.04 0 0.01 0.01 0 0.01 0.01 0.04 0 0.04
0.04
0 0.001 -0.001 0 0 0 0 0.001 -0.001 0.008 0 0 -
0.008 0 0 0.001 0 0.001 -0.001 0 -0.001 0.008 0.008
0.008 -0.008
0 0 0 0.001 -0.001 0 0 0.001 -0.001 0 0.008 0 0
-0.008 0 0.001 0.001 0 -0.001 -0.001 0 0 -0.008 0.008 -
0.008
0 0 0 0 0 0.001 -0.001 0.001 -0.001 0 0 0.008 0
0 -0.008 0 0.001 0.001 0 -0.001 -0.001 -0.008 0 0.008 -
0.008]';

```

```

y1=[515.0938547 431.9395619 598.2481475 615.6112589 414.5764506
418.0765437 625.4725059 435.4396551 594.7480544 348.7852691 716.128663
321.0592327 681.4024403 314.0590464 709.1284768 532.4569661 518.5939478
334.9222509 497.7307434 511.5937616 695.2654585 542.8198912 147.7504608
355.7854554 674.402254
]';
y2=[448.9524798 686.3242122 211.5807475 -6.02551545 903.9304751
997.5845856 -192.7615431 779.9783227 117.9266369 923.6959446 -
461.0035107 1546.216691 -25.79098492 1358.90847 -648.3117318
231.3462169 542.6065904 1234.956318 666.5587427 355.2983693 -337.0513584
-173.5682671 1833.651935 1111.004166 -213.099206
]';
y3=[414.5085502 -40.46944509 869.4865455 2845.831136 -2016.814036 -
5718.319554 6753.756212 -3741.974963 4570.992063 -495.4474404
5277.153722 -11851.14766 1324.464541 -4448.136622 12680.16476
2390.853141 -3286.996968 -6173.297549 -1561.836041 4116.014068
7002.314649 11770.20877 -5358.092613 -7898.458476 8727.475576
]';
y4=[-61.64931395 486.9827919 -610.2814198 -6194.477418 6071.17879
32107.84566 -32462.26213 26523.64967 -26646.94829 1035.614898 -
12327.30552 64277.34064 -1158.913526 12204.00689 -64400.63927 -
5645.845312 25975.01756 32656.47777 5522.546684 -26098.31619 -
32779.7764 -63303.37506 13301.27111 53108.94865 -53232.24728
]';
y5=[105.3883373 -142.4832128 353.2598874 4161.354446 -3950.577772 -
26382.89333 26698.08886 -22574.79877 22785.57545 -390.354763
8217.320555 -52871.175 601.1314376 -8006.54388 53081.95168 3913.482896 -
22326.92722 -26630.76488 -3702.706221 22537.7039 26841.54156
52586.20858 -8502.286981 -45254.98588 45465.76256
]';

B1=(x'*x)^-1)*x'*y1;
B2=(x'*x)^-1)*x'*y2;
B3=(x'*x)^-1)*x'*y3;
B4=(x'*x)^-1)*x'*y4;
B5=(x'*x)^-1)*x'*y5;

%Objective Functions and Constraints:
syms r R y
y=sym('y',[num_var 1]);
R=sym('R',[bearing_var 1]);
f=(y(1)^2+y(2)^2+y(3)^2); %initial point, est from graph
y0(1,:)= [0;0;0];
% R(1)=B1(1)+B1(2)*y(1)+B1(3)*y(2)+B1(4)*y(3);
% R(2)=B2(1)+B2(2)*y(1)+B2(3)*y(2)+B2(4)*y(3);
% R(3)=B3(1)+B3(2)*y(1)+B3(3)*y(2)+B3(4)*y(3);
% R(4)=B4(1)+B4(2)*y(1)+B4(3)*y(2)+B4(4)*y(3);
% R(5)=B5(1)+B5(2)*y(1)+B5(3)*y(2)+B5(4)*y(3);
%
R(1)=B1(1)+B1(2)*y(1)+B1(3)*y(2)+B1(4)*y(3)+B1(5)*y(1)^2+B1(6)*y(2)^2+B1(7)
)*y(3)^2;

```

```

%
R(2)=B2(1)+B2(2)*y(1)+B2(3)*y(2)+B2(4)*y(3)+B2(5)*y(1)^2+B2(6)*y(2)^2+B2(7)
)*y(3)^2;
%
R(3)=B3(1)+B3(2)*y(1)+B3(3)*y(2)+B3(4)*y(3)+B3(5)*y(1)^2+B3(6)*y(2)^2+B3(7)
)*y(3)^2;
%
R(4)=B4(1)+B4(2)*y(1)+B4(3)*y(2)+B4(4)*y(3)+B4(5)*y(1)^2+B4(6)*y(2)^2+B4(7)
)*y(3)^2;
%
R(5)=B5(1)+B5(2)*y(1)+B5(3)*y(2)+B5(4)*y(3)+B5(5)*y(1)^2+B5(6)*y(2)^2+B5(7)
)*y(3)^2;
R(1)=B1(1)+B1(2)*y(1)+B1(3)*y(2)+B1(4)*y(3)+B1(5)*y(1)^2+B1(6)*y(2)^2+B1(7)
)*y(3)^2+B1(8)*y(1)^3+B1(9)*y(2)^3+B1(10)*y(3)^3;
R(2)=B2(1)+B2(2)*y(1)+B2(3)*y(2)+B2(4)*y(3)+B2(5)*y(1)^2+B2(6)*y(2)^2+B2(7)
)*y(3)^2+B2(8)*y(1)^3+B2(9)*y(2)^3+B2(10)*y(3)^3;
R(3)=B3(1)+B3(2)*y(1)+B3(3)*y(2)+B3(4)*y(3)+B3(5)*y(1)^2+B3(6)*y(2)^2+B3(7)
)*y(3)^2+B3(8)*y(1)^3+B3(9)*y(2)^3+B3(10)*y(3)^3;
R(4)=B4(1)+B4(2)*y(1)+B4(3)*y(2)+B4(4)*y(3)+B4(5)*y(1)^2+B4(6)*y(2)^2+B4(7)
)*y(3)^2+B4(8)*y(1)^3+B4(9)*y(2)^3+B4(10)*y(3)^3;
R(5)=B5(1)+B5(2)*y(1)+B5(3)*y(2)+B5(4)*y(3)+B5(5)*y(1)^2+B5(6)*y(2)^2+B5(7)
)*y(3)^2+B5(8)*y(1)^3+B5(9)*y(2)^3+B5(10)*y(3)^3;

Mr=0; theta=1; %initial values, reset after receiving output from TK.
g(1)=(100-R(1))/Py;
g(2)=(100-R(2))/Py;
g(3)=(100-R(3))/Py; %bearing loads must be positive
g(4)=(100-R(4))/Py;
g(5)=(100-R(5))/Py;
g(6)=(R(1)-Py)/Py;
g(7)=(R(2)-Py)/Py; %Bearing Loads can not exceed yield load
g(8)=(R(3)-Py)/Py;
g(9)=(R(4)-Py)/Py;
g(10)=(R(5)-Py)/Py;
%g(11)=(theta-.0003)/.0003; %maximum allowable misalignment at stern
bearing
% h(1)=-P-Fs*L+R(1)+R(2)+R(3)+R(4)+R(5); %sum of forces and moments = 0.
% h(2)=-P*L-Fs*L^2/2+R(1)*(L-x1)+R(2)*(L-x2)+R(3)*(L-x3)+R(4)*(L-x4)+Mr;

stop_SD=0;
stop_ep=0;
ii=1;
% Exterior Penalty Loop
while stop_ep==0
    i=1;
    y_hist(i,:) = y0(ii,:);%sets y_hist to last y value from prev. DM
loop.

%read and write to "black box" (TK Solver)
dlmwrite('bearing_offsets.asc', 'd:', ' ');
dlmwrite('bearing_offsets.asc',y0(ii,:), '-append'); %writes initial
point to an ascii file
!ShaftModel.vbs &
% system('e:\Optimization\Shaft_Deflection_keane.tkw');

```

```

    pause(3); %Pauses while TK
solver for new reactions
    system('taskkill /F /IM cmd.exe'); %closes DOS
command window
    BR=dlmread('TKOutputs.asc', ',', 1, 0); %reads reaction
list from TK Solver
    T=dlmread('Theta.asc', ',', 1, 0); %reads entire
theta list
    theta=T(1,1); %Mapping TK solver output to Matlab from ascii
file
Reactions(1,:)=[BR(1,1) BR(1,2) BR(1,3) BR(1,4) BR(2,3)];
Mr=BR(2,1);

%Direct Method Counter, resets to 1 when new DM loop is initiated.
syms g_c h_c
%Direct Method Loop, Build Lagrangian function
while stop_SD==0
    %test to see if inequality constraints are met at current point
    for j = 1:g_eq
        test=double(subs(g(j),{y},{y_hist(i,)}));
        if test > 0
            g_c(j,:) = g(j);
        else
            g_c(j,:) = 0;
        end
    end
    %test to see if equality constraints are met at current point
    for k = 1:h_eq
        test=double(subs(h(k),{y},{y_hist(i,)}));
        if abs(test) > 0.1*eps_h
            h_c(k,:) = h(k);
        else
            h_c(k,:) = 0;
        end
    end
    %add non-zero constraints to the objective function
    phi_sym = f;
    for j=1:g_eq
        phi_sym=phi_sym+r*g_c(j,).^2;
    end
    for k=1:h_eq
        phi_sym=phi_sym+r*h_c(k,).^2;
    end
    %solve for phi at current point
    phi_hist(i,1) = double(subs(phi_sym,[y;r],[y_hist(i,): r_val(ii)]));
    %Find new gradient
    for p=1:num_var
        c(p,1)=diff(phi_sym,y(p));
        c_hist(i,p)=double(subs(c(p,1),[y;r],[y_hist(i,): r_val(ii)]));
    end
    d_hist(i,:)=-c_hist(i,); %Find new descent direction.
    d_norm=norm(d_hist(i,)); %Find norm of d.
    if d_norm < eps_SD %Test for convergence
        break
    else
        stop=0;
    end
end

```

```

    end
    %calculates next search point as a function of alpha which is unknown
    syms alpha
    phi_alpha=subs(phi_sym,[y;r],[(y_hist(i,:)+alpha*d_hist(i,:))
r_val(ii)]);
    %find the gradient of phi(a)
    dphidalpha=diff(phi_alpha,alpha);
    %solve for alpha by setting the gradient equal to zero
    alpha_solve=double(solve(dphidalpha));
    %eliminate negative and imaginary roots
    for n=1:size(alpha_solve,1);
        if alpha_solve(n,1) <= 0
            alpha_solve(n,1) = 1e6;
        elseif abs(imag(alpha_solve(n,1))) > 1e-6
            alpha_solve(n,1) = 1e6;
        end
    end
    %pick the smallest real root
    alpha_hist(i,1)=min(real(alpha_solve));
    %calculates optimum point/new x values
    y_hist(i+1,:)=y_hist(i,:) + alpha_hist(i,1)*d_hist(i,:);

i=i+1;
end %end of Direct Method Loop
%check to see if constraints are satisfied.
for j=1:g_eq
    test=double(subs(g(j),{y},{y_hist(i,:)}));
    if test > eps_g
        g_test(ii,j) = 1;
    else
        g_test(ii,j) = 0;
    end
end
if h_eq == 0
    h_test(ii,:) = 0;
end
for k=1:h_eq
    test=double(subs(h(k),{y},{y_hist(i,:)}));
    if abs(test) > eps_h
        h_test(ii,k) = 1;
    else
        h_test(ii,k) = 0;
    end
end
if norm(h_test(ii,:))==0 && norm(g_test(ii,:)) == 0
    break
end
y0(ii+1,:)=y_hist(i,:);
Reaction_values=double(subs(R,{y},{y_hist(i,:)}));
r_val(ii+1,1)=r_mult*r_val(ii,1);
ii=ii+1;
%clear y_hist d_hist alpha_hist c_hist phi_hist phi g_c h_c

end
dlmwrite('bearing_offsets.asc', 'd:', ' ');

```

```

    dlmwrite('bearing_offsets.asc',y_hist(i,:), '-append'); %writes initial
point to an ascii file
    !ShaftModel.vbs &
    % system('e:\Optimization\Shaft_Deflection_keane.tkw');
    pause(3); %Pauses while TK
solver for new reactions
    system('taskkill /F /IM cmd.exe'); %closes DOS
command window
    BR=dlmread('TKOutputs.asc', ',', 1, 0); %reads reaction
list from TK Solver
    T=dlmread('Theta.asc', ',', 1, 0); %reads entire
theta list
    theta=T(1,1); %Mapping TK solver output to Matlab from ascii
file
    Reactions(1,:)=[BR(1,1) BR(1,2) BR(1,3) BR(1,4) BR(2,3)];
y0
y_hist
d_hist
r_val
y_opt=y_hist(i,:)
Reactions
iterations=ii
toc

```

## Second Iterations with Revised Function Approximations

```

clear all
clc
tic

%Parameters
x1=19; %Horizontal Location for each bearing
x2=133;
x3=253;
x4=294;
P=220; %Propellor Load (lbs)
Fs=3.82896; %distributed load (shaft weight lbs/in)
L=314; %Length of beam 2 (inches)
E=26000000; %Modulus of Elasticity (psi)
sigma=87;
percent_contact=5; %percent contact with journal surface area
contact_area=pi()*5*18*percent_contact/100;
safety_factor=1.5;
Py=sigma*contact_area/safety_factor; %Yield Strength (psi)
num_var=3; % # of design variables
bearing_var=5;
g_eq=10; % # of inequality constraints
h_eq=0; % # of equality constraints
eps_h=.01; % Tolerance for Equality Constraints
eps_g=.001; % Tolerance for Inequality Constraints
eps_SD=.001; % Convergence Criteria
r_val(1)=1; % Initial Penalty Value
r_mult=10; % Penalty Multiplier

%2nd iteration experimental data. 25 Random points selected

```

```

% (.0027, -.013, -.002)
x=[1 1 1 1 1 1 1 1 1 1 1 1 1 1 1 1 1 1
1 1 1 1 1 1 1
-0.0425 -0.04 -0.045 -0.04 -0.044625 -0.04675 -0.0425 0 -
0.0425 -0.0425 0 0 -0.0212 -0.085 -0.06375 -0.028333333 -0.045
-0.04 -0.03 0 -0.05 -0.0451 -0.0425 -0.05 -0.0048
-0.0351 -0.03 -0.0375 -0.04 -0.036855 -0.03861 -0.0351 -0.0351 0
0 -0.0351 0 -0.0175 -0.0702 -0.05265 -0.0234 -0.0235 -0.03 -0.02
0 -0.04 -0.0351 -0.02 -0.03 -0.0351
-0.0048 -0.005 -0.0025 -0.0075 -0.00504 -0.00528 0 -0.0048 -
0.0048 0 0 -0.0048 -0.0024 -0.0096 -0.0072 -0.0032 -0.001 -0.01 -
0.01 0 0 -0.01 0 -0.0048 -0.0425
0.00180625 0.0016 0.002025 0.0016 0.001991391 0.002185563 0.00180625
0 0.00180625 0.00180625 0 0 0.00044944 0.007225 0.004064063
0.000802778 0.002025 0.0016 0.0009 0 0.0025 0.00203401 0.00180625
0.0025 0.00002304
0.00123201 0.0009 0.00140625 0.0016 0.001358291 0.001490732 0.00123201
0.00123201 0 0 0.00123201 0 0.00030625 0.00492804 0.002772023
0.00054756 0.00055225 0.0009 0.0004 0 0.0016 0.00123201 0.0004
0.0009 0.00123201
0.00002304 0.000025 0.00000625 0.00005625 2.54016E-05 2.78784E-05 0
0.00002304 0.00002304 0 0 0.00002304 0.00000576 0.00009216
0.00005184 0.00001024 0.000001 0.0001 0.0001 0 0 0.0001 0
0.00002304 0.00180625
-7.67656E-05 -0.000064 -0.000091125 -0.000064 -8.88658E-05 -
0.000102175 -7.67656E-05 0 -7.67656E-05 -7.67656E-05 0 0
-9.52813E-06 -0.000614125 -0.000259084 -2.27454E-05 -
0.000091125 -0.000064 -0.000027 0 -0.000125 -9.17339E-05 -
7.67656E-05 -0.000125 -1.10592E-07
-4.32436E-05 -0.000027 -5.27344E-05 -0.000064 -5.00598E-05 -
5.75572E-05 -4.32436E-05 -4.32436E-05 0 0 -4.32436E-05 0
-5.35938E-06 -0.000345948 -0.000145947 -1.28129E-05 -1.29779E-
05 -0.000027 -0.000008 0 -0.000064 -4.32436E-05 -0.000008
-0.000027 -4.32436E-05
-1.10592E-07 -0.000000125 -1.5625E-08 -4.21875E-07 -1.28024E-07
-1.47198E-07 0 -1.10592E-07 -1.10592E-07 0 0 -1.10592E-07
-1.3824E-08 -8.84736E-07 -3.73248E-07 -3.2768E-08 -0.000000001 -
0.000001 -0.000001 0 0 -0.000001 0 -1.10592E-07 -7.67656E-
05
]';

y1=[519.8096512 523.0512161 517.2446927 515.4249085 520.045441
520.2812309 515.1528203 484.4690768 555.0912601 550.4344292 479.8122459
519.7506856 517.4604345 524.5254477 522.1675495 518.2377188 529.8618696
527.9020817 529.6383928 515.0938547 516.4640394 527.016563 530.3309483
531.1726108 525.0360091
]';

y2=[481.4324288 463.0655802 499.0361458 494.847577 483.0564263
484.6804237 507.7667699 582.3154151 321.7351525 348.0694936 608.6497562
422.6181387 465.0836512 513.9123778 497.6724033 470.60578 443.5687081
435.6339749 413.8733486 448.9524798 512.2578117 446.7318943 439.0650926
440.4256711 364.087268
]';

y3=[48.85571944 173.7443777 -139.1766191 83.93282164 30.5730779
12.29043637 -245.5200295 -144.5099285 902.2499472 607.8741982 -
438.8856775 708.8842992 232.6703071 -316.7971113 -133.9706959

```

```

170.7399948 109.2161214 480.3857828 678.0202419 414.5085502 -330.5314866
379.5922087 121.609681 206.976521 2189.40521
]';
y4=[313.6689465 -49.72847407 1187.039403 -240.6830382 332.4348596
351.2007726 1857.804706 546.8375915 -1838.953718 -294.8179589
2090.97335 -1605.785073 123.2177183 688.987207 501.3280768
188.5628615 810.985893 -1658.203223 -2216.622823 -61.64931395
2117.165875 -1373.409227 931.7476618 -40.2526947 -11607.39636
]';
y5=[58.52716204 312.1612082 -641.8497142 568.771639 56.18410328
53.84104452 -1212.910358 -46.81824676 1482.171266 210.7337461 -
1318.255767 1376.825857 83.86179695 11.66598678 35.09657441 74.14755297
-471.338684 1636.575292 2017.384748 105.3883373 -1393.062331
1442.362469 -600.4594757 283.9717999 9951.161777
]';

B1=(x'*x)^-1*x'*y1;
B2=(x'*x)^-1*x'*y2;
B3=(x'*x)^-1*x'*y3;
B4=(x'*x)^-1*x'*y4;
B5=(x'*x)^-1*x'*y5;

%Objective Functions and Constraints:
syms r R y
y=sym('y',[num_var 1]);
R=sym('R',[bearing_var 1]);
f=(y(1)^2+y(2)^2+y(3)^2); %initial point, est from graph
y0(1,:)= [.0026;-.0129;-.0020];
R(1)=B1(1)+B1(2)*y(1)+B1(3)*y(2)+B1(4)*y(3)+B1(5)*y(1)^2+B1(6)*y(2)^2+B1(7)
)*y(3)^2+B1(8)*y(1)^3+B1(9)*y(2)^3+B1(10)*y(3)^3;
R(2)=B2(1)+B2(2)*y(1)+B2(3)*y(2)+B2(4)*y(3)+B2(5)*y(1)^2+B2(6)*y(2)^2+B2(7)
)*y(3)^2+B2(8)*y(1)^3+B2(9)*y(2)^3+B2(10)*y(3)^3;
R(3)=B3(1)+B3(2)*y(1)+B3(3)*y(2)+B3(4)*y(3)+B3(5)*y(1)^2+B3(6)*y(2)^2+B3(7)
)*y(3)^2+B3(8)*y(1)^3+B3(9)*y(2)^3+B3(10)*y(3)^3;
R(4)=B4(1)+B4(2)*y(1)+B4(3)*y(2)+B4(4)*y(3)+B4(5)*y(1)^2+B4(6)*y(2)^2+B4(7)
)*y(3)^2+B4(8)*y(1)^3+B4(9)*y(2)^3+B4(10)*y(3)^3;
R(5)=B5(1)+B5(2)*y(1)+B5(3)*y(2)+B5(4)*y(3)+B5(5)*y(1)^2+B5(6)*y(2)^2+B5(7)
)*y(3)^2+B5(8)*y(1)^3+B5(9)*y(2)^3+B5(10)*y(3)^3;

Mr=0; theta=1; %initial values, reset after receiving output from TK.
g(1)=(100-R(1))/Py;
g(2)=(100-R(2))/Py;
g(3)=(100-R(3))/Py; %bearing loads must be positive
g(4)=(100-R(4))/Py;
g(5)=(100-R(5))/Py;
g(6)=(R(1)-Py)/Py;
g(7)=(R(2)-Py)/Py; %Bearing Loads can not exceed yield load
g(8)=(R(3)-Py)/Py;
g(9)=(R(4)-Py)/Py;
g(10)=(R(5)-Py)/Py;
g(11)=(theta-.0003)/.0003;%maximum allowable misalignment at stern bearing
% h(1)=-P-Fs*L+R(1)+R(2)+R(3)+R(4)+R(5); %sum of forces and moments = 0.
% h(2)=-P*L-Fs*L^2/2+R(1)*(L-x1)+R(2)*(L-x2)+R(3)*(L-x3)+R(4)*(L-x4)+Mr;

stop_SD=0;

```

```

stop_ep=0;
ii=1;
% Exterior Penalty Loop
while stop_ep==0
    i=1;
    y_hist(i,:) = y0(ii,:);%sets y_hist to last y value from prev. DM
loop.

    %read and write to "black box" (TK Solver)
    dlmwrite('bearing_offsets.asc', 'd:', ' ');
    dlmwrite('bearing_offsets.asc',y0(ii,:),'-append');
    !ShaftModel.vbs &
    % system('e:\Optimization\Shaft_Deflection_keane.tkw');
    pause(3); %Pauses while TK solver for new
reactions
    system('taskkill /F /IM cmd.exe'); %closes DOS command
window
    BR=dlmread('TKOutputs.asc', ',', 1, 0);%reads reaction list from TK
Solver
    T=dlmread('Theta.asc', ',', 1, 0); %reads entire theta
list
    theta=T(1,1); %Mapping TK solver output to Matlab from ascii
file
    Reactions(1,:)=[BR(1,1) BR(1,2) BR(1,3) BR(1,4) BR(2,3)];
    Mr=BR(2,1);

    %Direct Method Counter, resets to 1 when new DM loop is initiated.
    syms g_c h_c
    %Direct Method Loop, Build Lagrangian function
    while stop_SD==0

        for j = 1:g_eq
            test=double(subs(g(j),{y},{y_hist(i,)}));
            if test > 0
                g_c(j,:) = g(j);
            else
                g_c(j,:) = 0;
            end
        end
        %test to see if equality constraints are met at current point
        for k = 1:h_eq
            test=double(subs(h(k),{y},{y_hist(i,)}));
            if abs(test) > 0.1*eps_h
                h_c(k,:) = h(k);
            else
                h_c(k,:) = 0;
            end
        end
        %add non-zero constraints to the objective function
        phi_sym = f;
        for j=1:g_eq
            phi_sym=phi_sym+r*g_c(j,).^2;
        end
        for k=1:h_eq
            phi_sym=phi_sym+r*h_c(k,).^2;

```

```

end
%solve for phi at current point
phi_hist(i,1) = double(subs(phi_sym,[y;r],[y_hist(i,:) r_val(ii)]));
%Find new gradient
for p=1:num_var
    c(p,1)=diff(phi_sym,y(p));
    c_hist(i,p)=double(subs(c(p,1),[y;r],[y_hist(i,:) r_val(ii)]));
end
d_hist(i,:)=-c_hist(i,:);      %Find new descent direction.
d_norm=norm(d_hist(i,:));      %Find norm of d.
if d_norm < eps_SD             %Test for convergence
    break
else
    stop=0;
end
%calculates next search point as a function of alpha which is unknown
syms alpha
phi_alpha=subs(phi_sym,[y;r],[(y_hist(i,:)+alpha*d_hist(i,:))
r_val(ii)]);
%find the gradient of phi(a)
dphialpha=diff(phi_alpha,alpha);
%solve for alpha by setting the gradient equal to zero
alpha_solve=double(solve(dphialpha));
%eliminate negative and imaginary roots
for n=1:size(alpha_solve,1);
    if alpha_solve(n,1) <= 0
        alpha_solve(n,1) = 1e6;
    elseif abs(imag(alpha_solve(n,1))) > 1e-6
        alpha_solve(n,1) = 1e6;
    end
end
%pick the smallest real root
alpha_hist(i,1)=min(real(alpha_solve));
%calculates optimum point/new x values
y_hist(i+1,:)=y_hist(i,:) + alpha_hist(i,1)*d_hist(i,:);

i=i+1;
end %end of Direct Method Loop
%check to see if constraints are satisfied.
for j=1:g_eq
    test=double(subs(g(j),{y},{y_hist(i,:)}));
    if test > eps_g
        g_test(ii,j) = 1;
    else
        g_test(ii,j) = 0;
    end
end
end
if h_eq == 0
    h_test(ii,:) = 0;
end
for k=1:h_eq
    test=double(subs(h(k),{y},{y_hist(i,:)}));
    if abs(test) > eps_h
        h_test(ii,k) = 1;
    else
        h_test(ii,k) = 0;
    end
end

```

```

        end
    end
    if norm(h_test(ii,:))==0 && norm(g_test(ii,:)) == 0
        break
    end
    y0(ii+1,:)=y_hist(i,:);
    Reaction_values=double(subs(R,{y},{y_hist(i,:)}));
    r_val(ii+1,1)=r_mult*r_val(ii,1);
    ii=ii+1;
    %clear y_hist d_hist alpha_hist c_hist phi_hist phi g_c h_c

end
%read final point into TK for final reactions
dlmwrite('bearing_offsets.asc', 'd:', ' ');
dlmwrite('bearing_offsets.asc',y_hist(i,:), '-append');
!ShaftModel.vbs &
% system('e:\Optimization\Shaft_Deflection_keane.tkw');
pause(3);
system('taskkill /F /IM cmd.exe');
BR=dlmread('TKOutputs.asc', ',', 1, 0);
T=dlmread('Theta.asc', ',', 1, 0);
theta=T(1,1);
Reactions(1,:)=[BR(1,1) BR(1,2) BR(1,3) BR(1,4) BR(2,3)];
y0
y_hist
d_hist
r_val
y_opt=y_hist(i,:)
Reactions
DM_interations=i
EPM_interations=ii
toc

```

## **Appendix C: Matrix used for Calculation in TKSolver Shaft Model**

This Appendix describes the Chapter 2 calculations in more detail. Specifically it shows the vectors and matrix used in the TKSolver program shown in Appendix A.

The following page shows the system of equations used to solve for the shaft's deflection, moment and slope at any point, arranged in the following format

$$\begin{array}{ccc} [\textit{Compliance Matrix}] * [\textit{Load Vector}] = [\textit{Deflection Vector}] \\ (8 \times 8) \qquad \qquad \qquad (8 \times 1) \qquad \qquad \qquad (8 \times 1) \end{array}$$

Nomenclature:

Expansion of the row 1, column 1 entry in the compliance matrix:

$$\int_0^L \frac{X1X1}{EI} dx$$

Since

$$(x - x_1) * H_{x_1} = X_1$$

And  $H_{x_i}$  is a heavy-side step function:

$$H_{x_i} = \begin{cases} 0, & x < x_i \\ 1, & x \geq x_i \end{cases}$$

The expanded form of the row 1, column 1 compliance matrix entry becomes:

$$\int_0^L \frac{X1X1}{EI} dx = \frac{1}{EI} * \int_0^L [(x - x_1) * H_{x_1}] * [(x - x_1) * H_{x_1}] dx$$

$\int_0^L \frac{X1X1dx}{EI}$	$\int_0^L \frac{X2X1dx}{EI}$	$\int_0^L \frac{X3X1dx}{EI}$	$\int_0^L \frac{X4X1dx}{EI}$	$(L - x1)$	0	1	0	R1	$\delta_1 + \int_0^L \left[ \frac{Px + \frac{1}{2} * Fs * x^2}{EI} \right] X1 dx$
$\int_0^L \frac{X1X2dx}{EI}$	$\int_0^L \frac{X2X2dx}{EI}$	$\int_0^L \frac{X3X2dx}{EI}$	$\int_0^L \frac{X4X2dx}{EI}$	$(L - x2)$	0	1	0	R2	$\delta_2 + \int_0^L \left[ \frac{Px + \frac{1}{2} * Fs * x^2}{EI} \right] X2 dx$
$\int_0^L \frac{X1X3dx}{EI}$	$\int_0^L \frac{X2X3dx}{EI}$	$\int_0^L \frac{X3X3dx}{EI}$	$\int_0^L \frac{X4X3dx}{EI}$	$(L - x3)$	0	1	0	R3	$\delta_3 + \int_0^L \left[ \frac{Px + \frac{1}{2} * Fs * x^2}{EI} \right] X3 dx$
$\int_0^L \frac{X1X4dx}{EI}$	$\int_0^L \frac{X2X4dx}{EI}$	$\int_0^L \frac{X3X4dx}{EI}$	$\int_0^L \frac{X4X4dx}{EI}$	$(L - x4)$	0	1	0	R4	$\delta_4 + \int_0^L \left[ \frac{Px + \frac{1}{2} * Fs * x^2}{EI} \right] X4 dx$
$(L - x1)$	$(L - x2)$	$(L - x3)$	$(L - x4)$	0	1	0	0	$\lambda 2$	$P * L + Fs * L^2 / 2$
0	0	0	0	1	$-\frac{1}{K_2}$	0	0	MR	0
1	1	1	1	0	0	0	1	$\lambda 1$	$P + Fs * L$
0	0	0	0	0	0	1	$-\frac{1}{K_1}$	RR	0

=